

NASA/TM—2011-215493



# Sources of Variation in Creep Testing

*William S. Loewenthal*  
*Ohio Aerospace Institute, Brook Park, Ohio*

*David L. Ellis*  
*Glenn Research Center, Cleveland, Ohio*

## NASA STI Program . . . in Profile

Since its founding, NASA has been dedicated to the advancement of aeronautics and space science. The NASA Scientific and Technical Information (STI) program plays a key part in helping NASA maintain this important role.

The NASA STI Program operates under the auspices of the Agency Chief Information Officer. It collects, organizes, provides for archiving, and disseminates NASA's STI. The NASA STI program provides access to the NASA Aeronautics and Space Database and its public interface, the NASA Technical Reports Server, thus providing one of the largest collections of aeronautical and space science STI in the world. Results are published in both non-NASA channels and by NASA in the NASA STI Report Series, which includes the following report types:

- **TECHNICAL PUBLICATION.** Reports of completed research or a major significant phase of research that present the results of NASA programs and include extensive data or theoretical analysis. Includes compilations of significant scientific and technical data and information deemed to be of continuing reference value. NASA counterpart of peer-reviewed formal professional papers but has less stringent limitations on manuscript length and extent of graphic presentations.
- **TECHNICAL MEMORANDUM.** Scientific and technical findings that are preliminary or of specialized interest, e.g., quick release reports, working papers, and bibliographies that contain minimal annotation. Does not contain extensive analysis.
- **CONTRACTOR REPORT.** Scientific and technical findings by NASA-sponsored contractors and grantees.

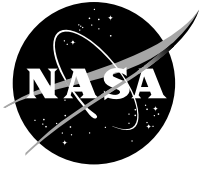
- **CONFERENCE PUBLICATION.** Collected papers from scientific and technical conferences, symposia, seminars, or other meetings sponsored or cosponsored by NASA.
- **SPECIAL PUBLICATION.** Scientific, technical, or historical information from NASA programs, projects, and missions, often concerned with subjects having substantial public interest.
- **TECHNICAL TRANSLATION.** English-language translations of foreign scientific and technical material pertinent to NASA's mission.

Specialized services also include creating custom thesauri, building customized databases, organizing and publishing research results.

For more information about the NASA STI program, see the following:

- Access the NASA STI program home page at <http://www.sti.nasa.gov>
- E-mail your question via the Internet to [help@sti.nasa.gov](mailto:help@sti.nasa.gov)
- Fax your question to the NASA STI Help Desk at 443-757-5803
- Telephone the NASA STI Help Desk at 443-757-5802
- Write to:  
NASA Center for AeroSpace Information (CASI)  
7115 Standard Drive  
Hanover, MD 21076-1320

NASA/TM—2011-215493



# Sources of Variation in Creep Testing

*William S. Loewenthal*  
*Ohio Aerospace Institute, Brook Park, Ohio*

*David L. Ellis*  
*Glenn Research Center, Cleveland, Ohio*

National Aeronautics and  
Space Administration

Glenn Research Center  
Cleveland, Ohio 44135

---

December 2011

## Acknowledgments

The authors acknowledge and express their appreciation to the efforts of Sharon Y. Thomas and John W. Zoha for conducting the creep testing and the important contributions by Ronald E. Phillips, John J. Juhas, and Adrienne H. Veverka for their help in identifying sources of equipment variation and quickly implementing the needed modifications.

Trade names and trademarks are used in this report for identification only. Their usage does not constitute an official endorsement, either expressed or implied, by the National Aeronautics and Space Administration.

*Level of Review:* This material has been technically reviewed by technical management.

Available from

NASA Center for Aerospace Information  
7115 Standard Drive  
Hanover, MD 21076-1320

National Technical Information Service  
5301 Shawnee Road  
Alexandria, VA 22312

Available electronically at <http://www.sti.nasa.gov>

# Sources of Variation in Creep Testing

William S. Loewenthal<sup>1</sup>  
Ohio Aerospace Institute  
Brook Park, Ohio 44142

David L. Ellis  
National Aeronautics and Space Administration  
Glenn Research Center  
Cleveland, Ohio 44135

## Summary

This report is a section of the final report on the GRCop-84 task of the Constellation Program and incorporates the results obtained between October 2000 and September 2005 when the program ended.

Creep rupture is an important material characteristic for the design of a variety of rocket engines, including those for reusable vehicles, the Earth Departure Stage (EDS), and the Lunar Surface Access Module (LSAM). It was observed during the earlier characterization of GRCop-84 that the complete data set had nearly 4 orders of magnitude of scatter. This large scatter may have confounded attempts to accurately determine how creep performance was influenced by manufacturing. It was unclear if this variation was from the testing, the material, or a combination of both. Sources of variation were examined for constant-load vacuum creep tests. Special attention was paid to the repeatability between creep tests conducted on different creep frames. Tests were conducted on identically processed specimens at the same specified stresses and temperatures.

It was found that significant differences existed between the five constant-load Brew creep test frames examined and that the specimen temperature was higher than the desired temperature by as much as 43 °C (77 °F). It was also observed that the top-to-bottom temperature profile varied as much as 44 °C (79 °F). Results showed that GRCop-84 creep behavior is more sensitive to small furnace temperature changes than was previously realized. The higher actual temperatures suggest that the previously collected data are a conservative prediction of creep rate and life.

Improved specimen temperature measurement and control were incorporated as part of an effort to minimize the temperature variations. To verify that these modifications decreased variation, additional tests were conducted, and the data between Brew vacuum creep test frames were shown to be comparable. The variation decreased to 1/2 order of magnitude from the previously observed 2 orders of magnitude for the baseline extruded GRCop-84 data set. Independent determination of creep rates by a step-loading method in a reference load frame closely matches the creep rates determined after the Brew modifications. Substituting a helium atmosphere for the vacuum tended to decrease the sample temperature gradient by improving heat transfer, but helium was not a significant improvement over vacuum.

## Introduction

Creep rupture behavior is an important material characteristic needed for the design of rocket engines. GRCop-84 (Cu-8 at.% Cr-4 at.% Nb), a Cu alloy developed by the NASA Glenn Research Center, has excellent elevated temperature strength, low cycle fatigue (LCF), and creep properties. This makes it an excellent replacement candidate for NARloy-Z (Cu-3 wt% Ag-0.5 wt% Zr), the current Space Shuttle Main Engine main combustion chamber liner material, and makes it competitive with many other high-conductivity Cu alloys (Ref. 1). Work to understand and optimize GRCop-84 has produced a large database of creep data, which are reported elsewhere in the final report (Ref. 2, to be published).

---

<sup>1</sup>William Loewenthal worked for the Ohio Aerospace Institute at the time that this research was done. He now works for H.C. Starck in Euclid, Ohio.

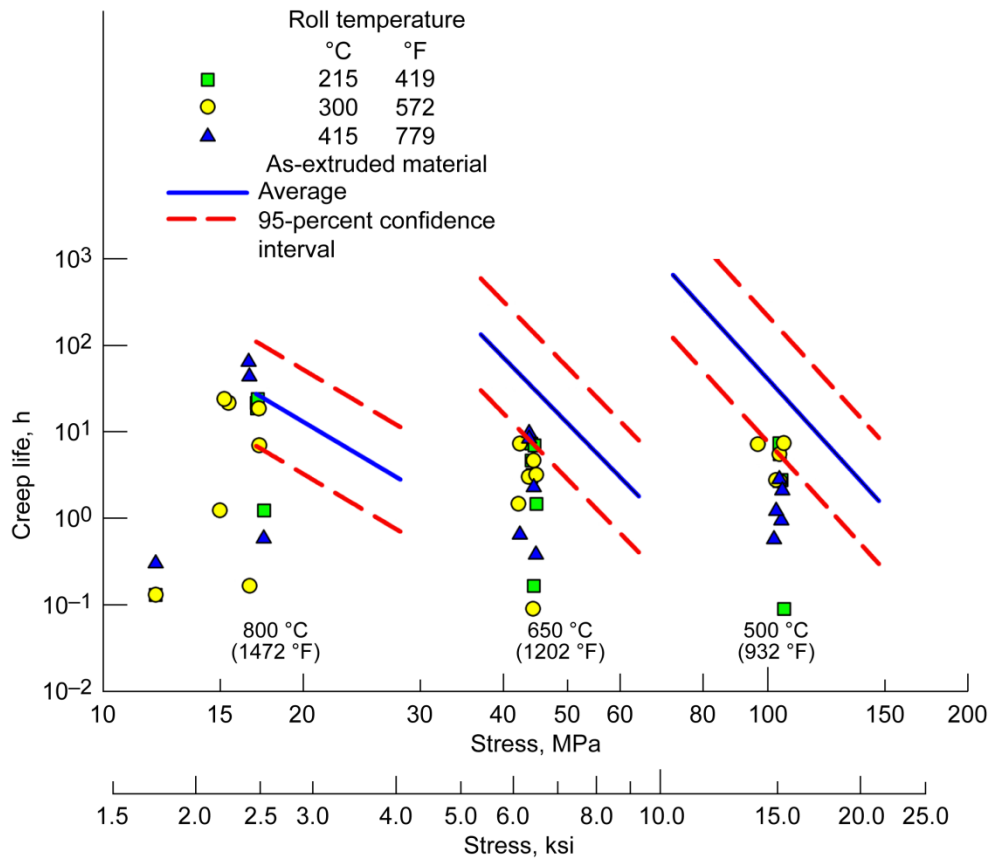


Figure 1.—Example of creep life scatter determined for warm rolled GRCop-84 sheet (Ref. 5).

It was observed that GRCop-84 creep data, regardless of process variants, consistently had nearly 2 orders of magnitude of scatter—even when tested on the same creep frame—and up to 4 orders of magnitude of scatter overall (Ref. 2 and Refs. 3 to 5). The large scatter has been an ongoing concern. One example showing large creep variation was observed during a study of GRCop-84 rolling parameters (Ref. 5). In this study, GRCop-84 sheet was rolled at 215, 300, and 415 °C (419, 572, and 779 °F), and creep life was determined at 500, 650, and 800 °C (932, 1202, and 1472 °F). The results shown in Figure 1 illustrate the large scatter, with considerable overlap of the results for the three rolling temperatures. Similarly, it is difficult to estimate the actual performance difference between the rolled sheet and the baseline extruded material (lines in Fig. 1). Although it appears that the rolled material has a lower creep life, the scatter does not allow such a conclusion to be reached statistically.

The problem is compounded when examining the complete historical data set. When all data are plotted as shown in Figure 2, the range of results approaches 4 orders of magnitude. However, the Monkman-Grant plot of the historical data had an excellent fit with only a few data points identified as probable outliers (Ref. 2). Given this variability within individual data sets and in the overall data, the statistical analysis was unable to detect significant differences between processing methods, heat treatments, or any other effects besides the primary ones of stress and temperature. Creep rate data are not presented, but the variability and range were almost identical to the creep lives presented in Figure 2.

It was unclear if this large variation was due to the test methods, the material, or a combination of both. Possible sources of variation besides material effects could include temperature and stress effects that were not accounted for in the original test method as well as instrumentation and calibration errors.

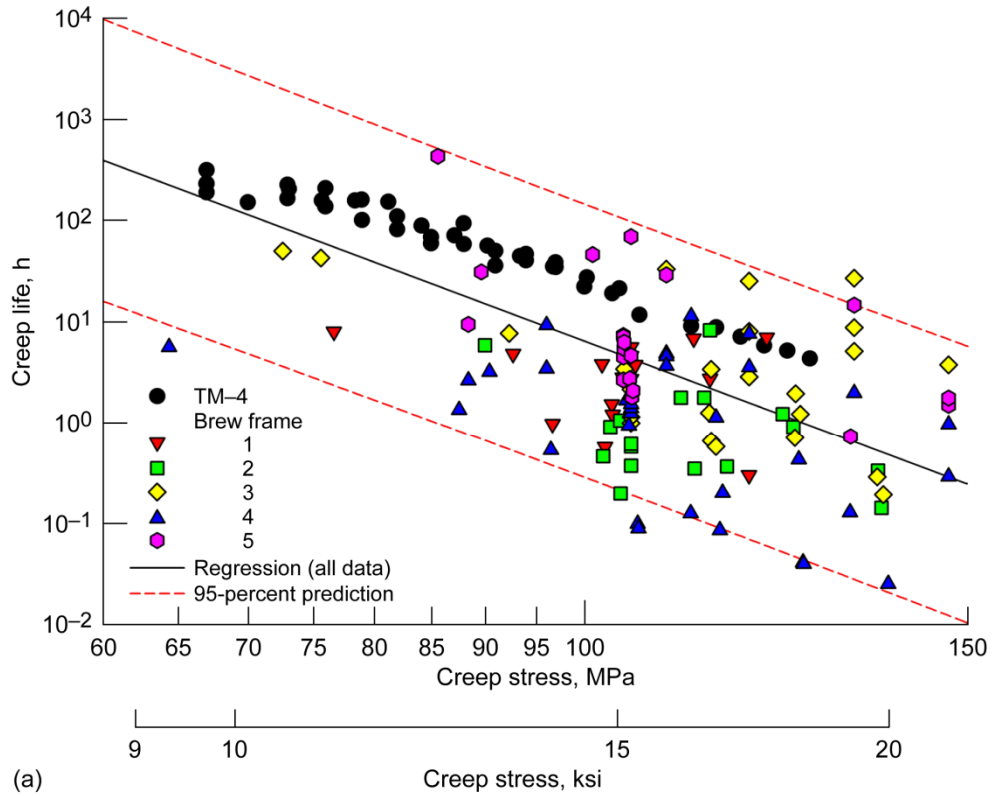


Figure 2.—Complete historical creep life data set with 95-percent confidence intervals.  
 (a) At 500 °C (932 °F).

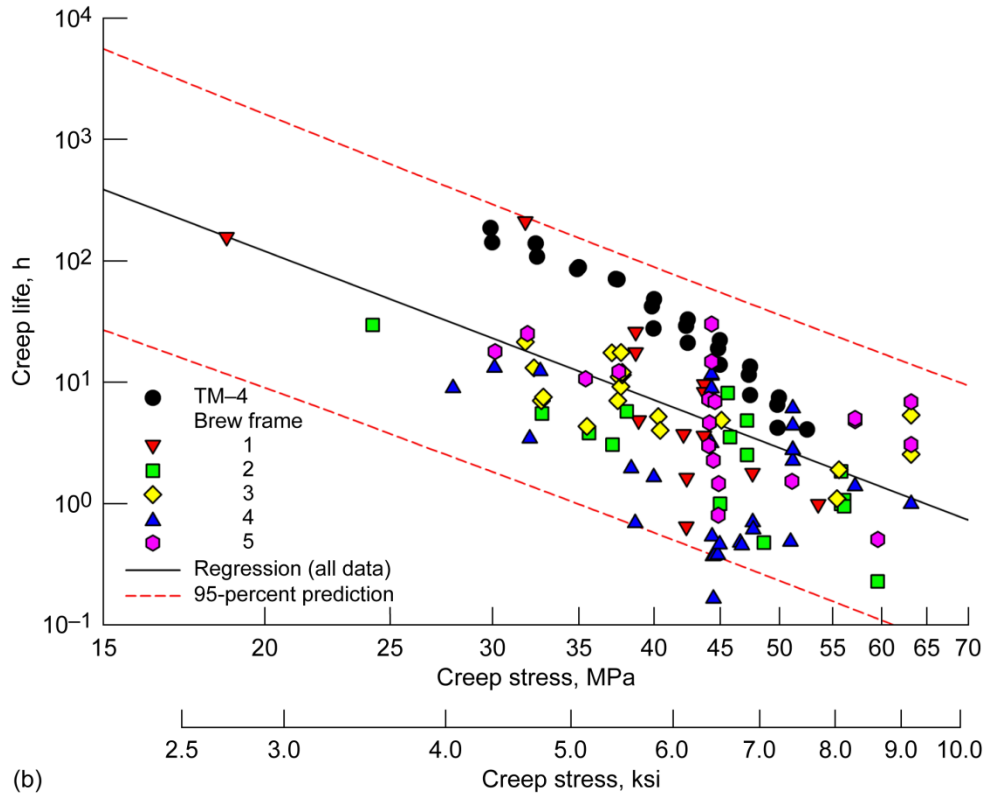


Figure 2.—Continued. (b) At 650 °C (1202 °F).

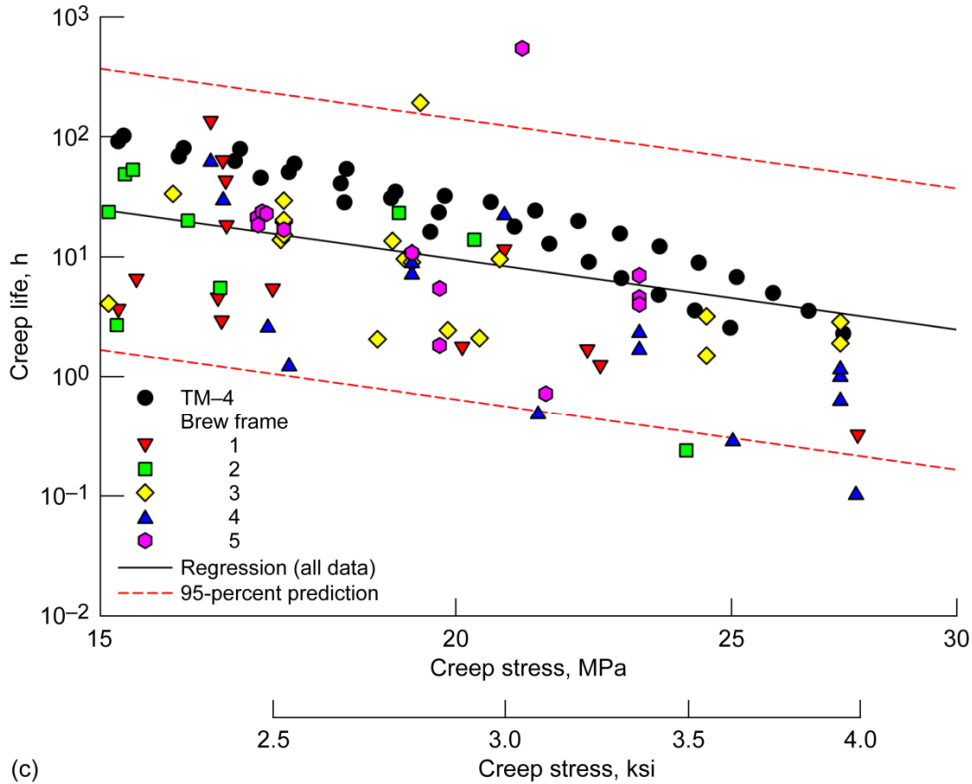


Figure 2.—Concluded. (c) At 800 °C (1472 °F).

Creep rupture lives and rates were measured under a constant load using a simple lever arm machine with a vacuum chamber manufactured by the Brew Corporation, referred to as a Brew test frame. These frames were manufactured circa 1957, have sequential serial numbers indicating manufacture at the same time, and had been upgraded once prior to the baseline GRCop-84 testing and twice prior to the current creep testing. The upgrades were designed to improve the data collection, temperature control, and vacuum systems by bringing them up to then current standards for electronics and data acquisition. All units were upgraded at the same time using the same components by the same technicians, so variation from frame to frame was anticipated to be minimal. However, the load, the load train alignment, the temperature, and other frame-specific variables were considered in this study.

From the baseline data shown in Figure 2, it was known that stress and temperature are the major factors affecting creep. Efforts were undertaken to experimentally characterize these and other potential machine-related factors affecting creep property variability through a design of experiments (DOE) and statistical analysis of the results.

## Experimental Procedure

GRCop-84 and other competitive materials were characterized in five of the six Brew frames available at Glenn. The Brew frames are numbered 1 to 6. Brew frame 6 (serial no. 31–309) was not used in these studies because of a nonfunctioning vacuum system. In addition, a calibrated data set for creep rate was created using a converted Instron tensile test frame (TM-4) whose load and temperature had been carefully characterized. The load measurement and temperature gradients were known to be superior for this unit. This data set was used as the baseline for determining the true creep rate of GRCop-84 at these temperatures and stresses.

Special attention was given to examining the repeatability between supposedly identical creep test conditions conducted on different Brew frames. So that the sources of variation between each Brew frame could be determined, a DOE was conducted on specimens from the same sheet of GRCop-84 at the same stresses and temperatures.

This work was conducted in three sequential stages, where the results of the prior stage were used to guide the work in the next stage. Details of the components of each stage are given following an overview.

In stage I, an initial survey was conducted to determine if the measured GRCop-84 creep properties for a single stress and temperature combination differed or were statistically the same between Brew frames. The findings from the initial survey confirmed that the mean value varied between Brew frames more than could be accounted for by the variation of results within a frame. This result led to a second stage to examine the potential sources of variation.

From the stage II (root cause) study, it was learned that variation in specimen temperature was larger and more important than previously recognized. Modifications were made to each Brew frame to monitor actual specimen temperature and thermal gradients by installing additional thermocouples. The operating procedure was also modified to control the furnace from the middle specimen thermocouple to achieve equivalent specimen temperatures for all tests in all Brew frames.

In stage III, the final stage, tests were conducted to validate that each Brew frame provided results similar to those of the other Brew frames and to the calibrated data set from TM-4. The updated procedures and test frames also were used to determine if the expected changes in creep properties with processing—which previously were not statistically significant, though probably observed—became statistically significant. The statistical variations of the results also were examined to determine if they had decreased.

### **Initial Survey Design of Experiments**

A DOE was conducted on identically processed specimens at the same applied stress and temperature combination to determine differences between creep test frames. It was assumed that conducting all of the creep tests from the same material lot would minimize any specimen-to-specimen differences; and that, if differences were observed, they could be attributed to the creep frame rather than to the material. Material effects were minimized further by taking the samples from random locations within a single sheet of material.

The test variables selected were Brew frame, temperature, and stress, with only the Brew frame purposely varied. From prior experience, the temperature and stress were well known to affect the creep rupture life of GRCop-84, as shown in Figures 1 and 2. It was suspected, but not known, that frame-to-frame variations existed despite the identical manufacture and operation of the units.

The response variables were creep life and creep rate. For the stage I survey to determine if there was variation between Brew frames, triplicate tests were conducted at 500 °C/105 MPa (932 °F/15.2 ksi) on each test frame for a total of 15 creep tests.

### **Investigation of Root Causes of Variation**

Various root causes that could produce different creep responses were investigated. These investigations centered on temperature and load, but other test aspects also were considered. A detailed evaluation was conducted of the creep test procedure, thermocouple and instrumentation calibration, frame alignment, friction in the mechanical feedthrough ball joints, and resistance from the weight of the rubber cooling hose hanging on the upper mechanical feedthrough ball joint. The procedure appeared to be adequate, the calibrations and alignments were good, and no extraneous loads or bending moments could be found. The results indicated that there were no major contributions from these factors, so the investigation of root causes which is reported here focuses on temperature and load.

During the investigation of root causes, thermocouples were installed on Brew frames 3 and 4 to monitor the specimen temperature and thermal gradients. These values were compared with the control thermocouple to determine variations between the control thermocouple and the sample temperature. Three thermocouples attached to the sample allowed measurement of the thermal gradients in the samples as well. Also on Brew frames 3 and 4, an 8.9-kN- (2000-lb<sub>f</sub>) capacity Sensotec model 31 series load cell and Model GM controller from Honeywell International Inc. were installed in the lower pull rod to examine loads and determine gross variations in the loads applied to the samples because of mechanical differences in the load frames.

The Brew frame test chambers were designed to allow pressurization of up to 1 atm as well as vacuum operation. An Omega Engineering DPF60 series controller and automated supply and bleed solenoid valves were added to Brew frame 3 to pressurize the chamber to 89.7 kPa (13 psi) with high-purity helium. It was thought that a helium atmosphere would improve specimen temperature uniformity by allowing heat transfer by convection as well as radiation and conduction within the sample. Helium was selected over argon and other inert gases because of its higher thermal conductivity. A series of tests using the GRCop-84 sheet samples shown in Table I were conducted following the same setup and test procedures used previously. The testing was conducted sequentially, except for tests 10 to 15, with the results of prior tests being used to determine the conditions to be used on the subsequent tests.

Results were analyzed using analysis of variance (ANOVA) tests to compare the average creep rate and creep life for the five test frames simultaneously. When differences in the means were detected, a Student-Newman-Keuls (SNK) test was used to compare and rank the means.

TABLE I.—SPECIMEN TEST CONDITIONS FOR INVESTIGATING ROOT CAUSES OF VARIATION

Test	Creep temperature		Creep stress		Brew frame	Atmosphere
	°C	°F	MPa	ksi		
1	500	932	105	15.2	3	Vacuum
2	500	932	105	15.2	3	Vacuum
3	500	932	105	15.2	4	Vacuum
4	800	1472	17	2.5	3	Vacuum
5	800	1472	17	2.5	4	Vacuum
6	650	1202	44.3	6.9	3	Vacuum
7	650	1202	44.3	6.9	4	Vacuum
8	500	932	105	15.2	3	Vacuum
9	500	932	105	15.2	4	Vacuum
10	500	932	105	15.2	3	Helium
11	500	932	105	15.2	3	Helium
12	650	1202	44.3	6.9	3	Helium
13	650	1202	44.3	6.9	3	Helium
14	800	1472	17	2.5	3	Helium
15	800	1472	17	2.5	3	Helium

### Designs of Experiments for Verifying Improvements

The stage II root cause determination found that temperature was the most important variable and that there were large differences between the control thermocouple temperature and the sample temperature. Furthermore, the differences did not appear to be consistent even within a single load frame. Thermocouples to measure the temperature of the top, middle, and bottom of the reduced section of the specimen were permanently installed in all Brew frames. The middle thermocouple temperature was used to control the temperature of the specimen after installation. The operating procedure was updated to include the newly determined best practices, including the use of three thermocouples for temperature measurement.

After these changes, another series of tests with GRCo-84 sheet specimens was conducted to confirm that the variation in creep properties was reduced and that the experimental error had been minimized. Duplicate tests of material from sheet 3A1B were measured at test conditions similar to those for historical tests. Creep conditions of 500 °C/105 MPa (932 °F/15.2 ksi), 650 °C/44.3 MPa (1202 °F/6.9 ksi), and 800 °C/17 MPa (1472 °F/2.5 ksi) were tested on Brew frames 2, 3, and 4. Brew frames 1, 5, and 6 were unavailable because of other testing. An additional series of tests was conducted at the same conditions except that a helium atmosphere was used instead of a vacuum and that the material came from sheet 4A2. Table II presents the verification test matrix.

TABLE II.—CONDITIONS AND SAMPLES FOR GRCo-84 SHEET VERIFICATION SURVEY DESIGN OF EXPERIMENTS

Run	Sample	Creep stress, MPa	Temperature, °C	Run	Sample	Creep stress, MPa	Temperature, °C
Vacuum tests				Helium atmosphere tests			
1	3BA1-1	105	500	1	4A2-1	105	500
2	3BA1-2	105	500	2	4A2-2	105	500
3	3BA1-3	44.3	650	3	4A2-3	44.3	650
4	3BA1-4	44.3	650	4	4A2-4	44.3	650
5	3BA1-5	17	800	5	4A2-5	17	800
6	3BA1-6	17	800	6	4A2-6	17	800
7	3BA1-7	105	500	7	4A2-7	105	500
8	3BA1-8	105	500	8	4A2-8	105	500
9	3BA1-9	44.3	650	9	4A2-9	44.3	650
10	3BA1-10	44.3	650	10	4A2-10	44.3	650
11	3BA1-11	17	800	11	4A2-11	17	800
12	3BA1-12	17	800	12	4A2-12	17	800
13	3BA1-13	105	500	13	4A2-13	105	500
14	3BA1-14	105	500	14	4A2-14	105	500
15	3BA1-15	44.3	650	15	4A2-15	44.3	650
16	3BA1-16	44.3	650	16	4A2-16	44.3	650
17	3BA1-17	17	800	17	4A2-17	17	800
18	3BA1-18	17	800	18	4A2-18	17	800

Two additional sets of creep tests were completed using the updated practices. The first was a survey of the creep properties of GRCo-84 plate made from standard -140 mesh powder. The second was an analysis of the effects of a braze thermal cycle on the creep properties of GRCo-42 (Cu-4 at.% Cr-2 at.% Nb).

The -140 mesh powder GRCo-84 plate is from material used in the production of several 177.9-kN (40 000-lb<sub>f</sub>) class rocket engine main combustion chamber liners and was used to verify and certify the liner material's creep properties. It provides a set of data for comparison of the observed variation in creep test results with a reasonably large data set. As such it provides an estimate of the material and remaining test method variability. Table III shows the test conditions and DOE.

Following testing, a model with the form

$$\log_{10}(Y) = \beta_0 + \beta_1 \log_{10}(\sigma) + \frac{\beta_2}{T + 273} + \beta_3 \frac{\log_{10}(\sigma)}{T + 273} \quad (1)$$

was entertained to determine the dependency of the dependent variable  $Y$  (creep rate in reciprocal seconds ( $s^{-1}$ ) or creep life in hours) on the stress  $\sigma$  and test temperature  $T$ . Here  $\beta_0$  to  $\beta_3$  are the coefficients to be fit by the regression analysis. Equation (1) allows prediction of the life and rate for intermediate temperatures and stresses, so it can be used to explore the relative dependency of the rate and life on these independent variables.

TABLE III.—CONDITIONS AND SAMPLES FOR GRCo-84 SHEET VERIFICATION

SURVEY DESIGN OF EXPERIMENTS

Run	Sample	Creep stress, MPa	Temperature, °C	Run	Sample	Creep stress, MPa	Temperature, °C
Vacuum tests				Helium atmosphere tests			
1	3BA1-1	105	500	1	4A2-1	105	500
2	3BA1-2	105	500	2	4A2-2	105	500
3	3BA1-3	44.3	650	3	4A2-3	44.3	650
4	3BA1-4	44.3	650	4	4A2-4	44.3	650
5	3BA1-5	17	800	5	4A2-5	17	800
6	3BA1-6	17	800	6	4A2-6	17	800
7	3BA1-7	105	500	7	4A2-7	105	500
8	3BA1-8	105	500	8	4A2-8	105	500
9	3BA1-9	44.3	650	9	4A2-9	44.3	650
10	3BA1-10	44.3	650	10	4A2-10	44.3	650
11	3BA1-11	17	800	11	4A2-11	17	800
12	3BA1-12	17	800	12	4A2-12	17	800
13	3BA1-13	105	500	13	4A2-13	105	500
14	3BA1-14	105	500	14	4A2-14	105	500
15	3BA1-15	44.3	650	15	4A2-15	44.3	650
16	3BA1-16	44.3	650	16	4A2-16	44.3	650
17	3BA1-17	17	800	17	4A2-17	17	800
18	3BA1-18	17	800	18	4A2-18	17	800

Three sets of GRCop-42 samples from the baseline extruded material (extrusion lots 192 and 211) were tested in the as-extruded condition and following simulated braze cycles at 935 and 1000 °C (1715 and 1832 °F). These simulated braze cycles are detailed in Tables IV and V. The objective of the test program was to determine if the creep rate increased and the creep life decreased as was expected from a decrease in tensile strength. Prior statistical analysis had not been able to detect such a difference even though the simulated braze cycle material tended to have the expected differences. The likely cause of the failure to detect the difference was the scatter in the data. With reduced scatter, it was expected that the differences would now be detectable if the changes had actually improved the test results. Such a result would validate the new test procedures.

Tests were conducted at 500, 650, and 800 °C (932, 1202, and 1472 °F) using multiple stresses. Table VI lists the test details. Following testing, a model was entertained to determine which independent variables were statistically significant. The model had the form

$$\log_{10}(Y) = \beta_0 + \beta_1 \log_{10}(\sigma) + \frac{\beta_2}{T + 273} + \beta_3 \frac{\log_{10}(\sigma)}{T + 273} + \beta_4 B_1 \log_{10}(\sigma) + \beta_5 B_2 \log_{10}(\sigma) + \frac{\beta_6 B_1}{T + 273} + \frac{\beta_7 B_2}{T + 273} \quad (2)$$

where  $Y$  is the dependent response variable (creep life in hours or creep rate in reciprocal seconds ( $s^{-1}$ ));  $\sigma$  is the applied stress in megapascals (MPa);  $T$  is the temperature in degrees Celsius;  $B_1$  and  $B_2$  are blocking variables corresponding to simulated brazes of 935 and 1000 °C, respectively; and  $\beta_0$  to  $\beta_7$  are the coefficients determined by the regression analysis.

A blocking variable took a value of 1 if the sample had a particular heat treatment and 0 if it did not. If both  $B_1$  and  $B_2$  were 0, the sample was in the as-extruded condition. The blocking variables allowed the use of forward stepwise regression to determine if a heat treatment had a significant effect. If no term with the blocking variable corresponding to a heat treatment entered the regression, the conclusion was that the heat treatment did not have a significant effect on creep properties relative to the as-extruded condition.

TABLE IV.—SIMULATED 935 °C (1715 °F) BRAZE CYCLE

Step	Temperatures and rates	
	°C at °C/min	°F at °F/min
1	Room temperature to 538 °C at 5.6 °C/min	Room temperature to 1000 °F at 10 °F/min
2	538 to 871 °C at 2.8 °C/min	1000 to 1600 °F at 5 °F/min
3	871 to 935 °C at 1.7 °C/min	1600 to 1715 °F at 3 °F/min
4	935±8.3 °C/hold for 22.5±2.5 min	1715±15 °F/hold for 22.5±2.5 min
5	935 to 871 °C at 1.7 °C/min	1715 to 1600 °F at 3 °F/min
6	871 to 538 °C at 2.8 °C/min	1600 to 1000 °F at 5 °F/min
7	538 °C to room temperature free cool	1000 °F to room temperature free cool

TABLE V.—SIMULATED 1000 °C (1832 °F) BRAZE CYCLE

Step	Temperatures and rates	
	°C at °C/min	°F at °F/min
1	Room temperature to 538 °C at 5.6 °C/min	Room temperature to 1000 °F at 10 °F/min
2	538 to 816 °C at 2.8 °C/min	1000 to 1500 °F at 5 °F/min
3	816 to 1000 °C at 1.7 °C/min	1500 to 1832 °F at 3 °F/min
4	1000±8.3 °C/hold for 22.5±2.5 min	1832±15 °F/hold for 22.5±2.5 min
5	1000 to 260 °C at 2.8 °C/min	1832 °F to 500 °F at 5 °F/min
6	260 to 121 °C at 2.8 °C/min or best possible cooling rate	500 to 250 °F at 5 °F/min or best possible cooling rate
7	121 °C to room temperature free cool	250 °F to room temperature free cool

TABLE VI.—CONDITIONS AND SAMPLES FOR GRCop-42 BRAZE EFFECT DESIGN OF EXPERIMENTS

Run	Sample	Condition	Temperature, °C	Applied stress, MPa	Run	Sample	Condition	Temperature, °C	Applied stress, MPa
1	5-23	1000 °C braze	500	77.3	27	5-15	1000 °C braze	800	17.4
2	2-5	1000 °C braze	500	77.3	28	2-7	1000 °C braze	800	18.6
3	4-13	935 °C braze	500	70.7	29	4-12	935 °C braze	800	18.7
4	6-5	As extruded	500	97.8	30	1-22	As extruded	800	20.4
5	1-24	As extruded	500	92.0	31	4-11	935 °C braze	800	19.9
6	2-8	1000 °C braze	500	87.6	32	6-6	As extruded	800	21.8
7	3-5	935 °C braze	500	87.0	33	6-1	As extruded	800	20.4
8	5-19	1000 °C braze	500	82.4	34	4-25	935 °C braze	800	18.7
9	1-28	As extruded	500	97.8	35	1-17	As extruded	800	21.8
10	3-3	935 °C braze	500	92.5	36	3-1	935 °C braze	800	19.9
11	1-26	As extruded	500	92.0	37	5-24	1000 °C braze	650	35.0
12	3-4	935 °C braze	500	87.0	38	5-13	1000 °C braze	650	35.0
13	2-2	1000 °C braze	650	51.5	39	3-6	935 °C braze	650	35.0
14	1-23	As extruded	650	60.4	40	1-32	As extruded	650	35.0
15	1-16	As extruded	650	56.8	41	1-13	1000 °C braze	650	35.0
16	5-27	1000 °C braze	650	48.5	42	5-21	1000 °C braze	800	10.0
17	4-29	935 °C braze	650	49.7	43	6-7	As extruded	800	10.0
18	4-14	935 °C braze	650	53.0	44	4-19	935 °C braze	650	35.0
19	3-7	935 °C braze	650	49.7	45	5-28	1000 °C braze	500	130.0
20	1-19	As extruded	650	53.3	46	4-18	935 °C braze	800	10.0
21	2-4	1000 °C braze	650	45.5	47	1-31	As extruded	500	130.0
22	2-3	1000 °C braze	650	48.5	48	5-25	1000 °C braze	800	13.0
23	1-25	As extruded	650	56.8	49	5-26	1000 °C braze	800	10.0
24	4-28	935 °C braze	650	53.0	50	4-15	935 °C braze	500	130.0
25	5-16	1000 °C braze	800	17.4	51	1-18	As extruded	800	13.0
26	5-18	1000 °C braze	800	18.6	52	4-27	935 °C braze	800	13.0

Stepwise forward analysis was conducted using Systat Software's<sup>2</sup> SigmaStat Version 3.1 statistical software. The raw data were converted to the form needed for Equation (2), and blocking variables were added. Analyses were conducted for both the creep rate and creep life. The stepwise regression analysis used  $F$  statistic values (the value of the  $F$  distribution for  $X$  degrees of freedom associated with the numerator and  $Y$  degrees of freedom associated with the denominator) of 4 to enter and 3.9 to leave. These values were selected because they correspond to approximately a 95-percent probability that the variable should or should not be in the model, respectively.

### Specimen Designs

Quantities of standard sheet tensile specimens conforming to ASTM Standard E8 (Ref. 6) were wire electrical discharge machined. The sheet specimen design used is shown in Figure 3. The sheet samples for stages I and II of the study were commercially rolled by H.C. Starck GmbH in Coldwater, Michigan, to a nominal thickness of 0.762 mm (0.030 in.) and were annealed for 30 min at 600 °C (1112 °F). Details of the manufacturing process are reported in Reference 7. The stage II testing used materials from the rolling parameter optimizations study (Ref. 5). Neither set of samples had the recast layer removed because the volume of affected material was very small relative to the total volume and because the recast layer and base material should have similar microstructures since they were both rapidly solidified. In this context, the small amount of recast material was deemed unlikely to affect the test results. The procedure is also consistent with the preparation of prior test specimens.

The GRCop-42 bar stock used for creep testing was made by extruding two 22.7-kg (50-lb) lots of -140 mesh loose powder at H.C. Starck. The lots were designated 192 and 211. A nominal 30:1 reduction in area was used to produce 2.5-cm- (1-in.-) diameter rods. The GRCop-84 plate was made by extruding 800 lb of -140 mesh powder and rolling the material to 12.7-mm- (0.5-in.-) thick plate. Round samples conforming to ASTM Standard E8 were machined from the rods and plate for creep testing. The design used for these samples is shown in Figure 4.

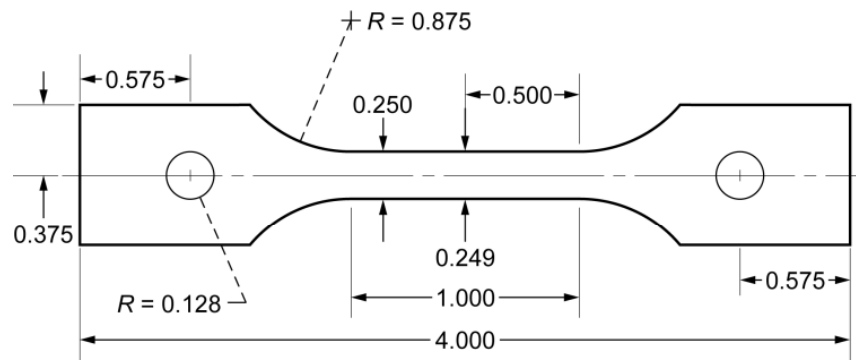


Figure 3.—Sheet specimen design used for creep and tensile tests. All dimensions given in inches.  $R$ , radius.

<sup>2</sup>Systat Software, Inc., 1735, Technology Drive, Ste. 430, San Jose, CA 95110.

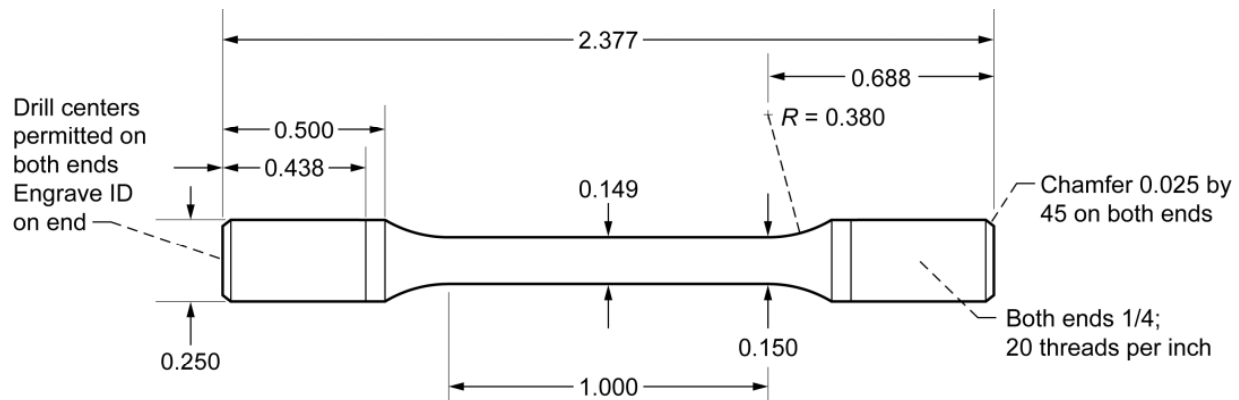


Figure 4.—Round specimen design used for GRCop-84 plate and GRCop-42 extrusion verification creep tests. All dimensions given in inches.  $R$ , radius.

## Creep Testing

Two types of creep tests were conducted: constant-load creep rupture tests and step-loading creep rate tests. Constant-load creep tests give a steady-state creep rate for a given stress and temperature as well as a rupture life. These were the tests conducted in the Brew frames. The step-loading tests were conducted using a separate modified tensile test load frame designated TM-4 with vacuum, heating, and data collection capabilities similar to those of the Brew frames. Step-loading tests produce many creep rates at different stresses but do not produce any creep lives. The procedures for conducting both types of creep tests are discussed in the following sections.

**Constant-load vacuum creep testing.**—Constant-load creep tests were conducted using a simple lever arm machine with a vacuum chamber. As noted before, the units were manufactured by the Brew Corporation circa 1957 and have undergone multiple upgrades to the electronics and controls since then. The current configuration is shown in Figure 5.

The test specimens were placed into a water-cooled stainless steel chamber with vacuum-tight mechanical feedthrough ball joints at the top and bottom. The ball joints ensure transmission of the load to the specimen with a minimal bending moment or other misalignments. The specimen was heated by a tungsten mesh heater surrounded by multiple tungsten heat shields. For GRCop-84 and GRCop-42 testing, Type 310 stainless steel fixtures were normally used, although MAR M-246 fixtures were used when 310 stainless steel fixtures were not available. The fixturing was adjusted in length so that the sample was centered in the hot zone.

Temperature control was initially done using an Inconel sheathed Type R (Pt/Pt-13% Rh) thermocouple with an exposed bead introduced through the back of the chamber. The control thermocouple was placed 1.6 to 3.2 mm (0.063 to 0.125 in.) from the sample. The thermocouple was not allowed to touch the specimen to prevent the development of a bending moment upon heating the specimen. An over-temperature thermocouple was coaxially located with the control thermocouple.

During this program, three additional flexible Type R thermocouples were attached to the top, middle, and bottom of the gauge section of the sample as shown in Figure 5(c). The thermocouples used high-purity, high-density alumina beads for insulation and sheathing. The beads also allowed the thermocouples to flex easily. Initially, these attached thermocouples were used only for sample temperature measurements. Later, the middle thermocouple also was used as the control thermocouple for stage III, the final stage of the study, when the improved testing procedures were verified. A vacuum-tight thermocouple feedthrough was used to connect the thermocouples to exterior instrumentation and data acquisition.

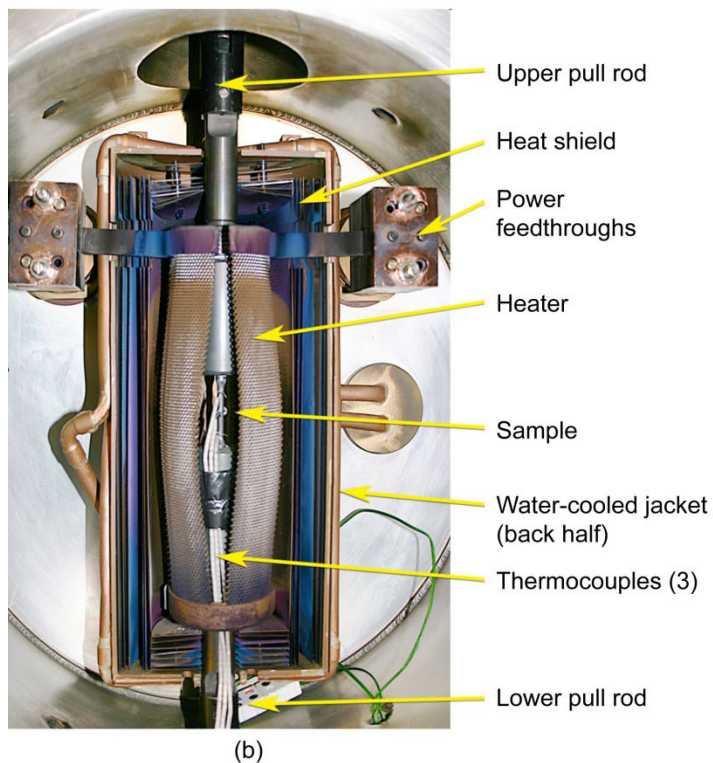
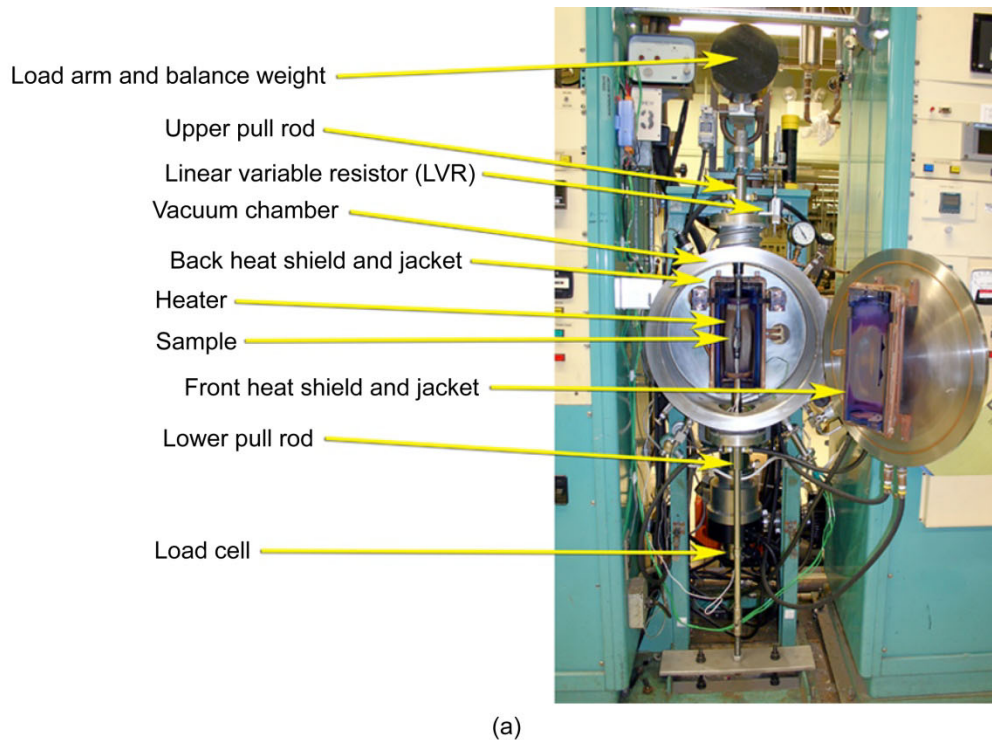


Figure 5.—Brew constant-load creep-test frame. (a) View of frame and chamber. (b) View inside chamber. (c) Thermocouples attached to specimen.

The load was applied to the specimen using a 10:1 lever arm and a dead weight consisting of various size weights. A load pan was attached to the opposite end of the lever arm from the sample to allow the weights to be stacked. Prior to loading the sample, the arm was leveled and balanced so that no moments or loads were induced in the samples from the lever arm. The samples were heated in vacuum to the desired test temperature with a minimal load (typically 4.5 N or 1 lb<sub>f</sub>) to stabilize the sample and fixtures during heating. When the sample's temperature stabilized, a scissor jack was raised underneath the pan to remove all weight on the lever arm, the desired pan load equal to 1/10 the desired sample load was placed on the pan, and the scissor jack was lowered. The load on the sample was measured using an 8.9-kN- (2000-lb<sub>f</sub>-) capacity Honeywell Sensotec Type 31 miniature load cell placed in the load train beneath the chamber during tests where the load cell had been added to the test frames. The load cell allowed a quantitative measure of the load and acted as a way for the data acquisition system to detect failure of the sample. The maximum error for the load cells based on the manufacturer-supplied specifications was 0.25 percent of full scale, or 22 N (5 lb<sub>f</sub>).

Displacement was measured by a linear variable resistor (LVR) attached to the load train rather than the sample. The LVR used has a resolution of 2.54 μm (0.0001 in.) and, unlike prior optical measurements, allowed the displacement to be recorded at a frequent, set time interval. So that the strain could be calculated, the gauge length of the reduced section was measured using a Focus Contour Projector optical comparator from Optical Gaging Products, Inc. The displacement measured by the LVR was divided by the initial room temperature gauge length to compute the strain.

At least the first data point included the displacement caused by the slack of the load frame being removed through the application of the load. No adjustments to the LVR displacement values and measured strain were made for the loading displacement because there was no direct measurement of the sample displacement from which to assign definitive values to the duration and magnitude of the loading displacement. Prior in-house efforts to measure the strain in the reduced section using an optical cathetometer and to correlate the LVR strains to sample strains showed that there was a strong correlation between the two measurements, but the scatter in the data was too great to provide the degree of confidence desired for conversion of the LVR strain into sample strain and ultimately creep strain (Ref. 2, to be published).

The correlation and the individual creep curves generated for the samples used to develop the correlation did show that the relative displacements measured by the LVRs between consecutive data points accurately represented the actual change in the sample's strain as measured by the cathetometers. Because of this, the absolute magnitude of the LVR strain without any adjustments was uncertain and inaccurate, but the change in strain after the first few data points was accurate. Since the steady-state creep rate was calculated from the relative change of the strains well after the initial loading, the creep rate was accurate.

All signals were collected by data acquisition using internally developed NASA data acquisition software running on a Dell 2400 desktop computer. The signals were converted from analog to digital using I-7019R eight-channel universal analog input modules from MicroDAQ.com, Ltd., connected to an I-7561 USB (universal serial bus) to an RS-232/422/485 converter. Data were collected every second for the first 5 min of the test, every 5 min for the next 30 min of the test, and once every hour until the end of the test. In addition, the software queried the modules once every 10 s and stored the data in a ring buffer. Upon failure, as defined by a 90-percent or more drop in the load from the peak load, the contents of the ring buffer were written to the file, and the 10-s-interval data for the last hour of the test were recorded.

During testing, using a helium atmosphere instead of vacuum was investigated to determine if it would improve specimen temperature uniformity. An Omega Engineering DPF60 series process controller was used to control the helium pressure into the chamber. An electrically operated inlet and outlet solenoid valve and a pressure transducer were connected to the process controller. The process controller was set to maintain 93- to 97-Pa (13.5- to 14-psia) pressure in the chamber as measured by the pressure transducer. The outlet line had to be connected to an existing mechanical vacuum pump to remove extra helium since the chamber pressure was slightly below 1 atm. This design resulted in a very low flow of helium through the chamber and hence very little temperature fluctuation due to the sudden inrush of gas. The selected system also had the advantage of minimizing oxygen contamination and helium usage.

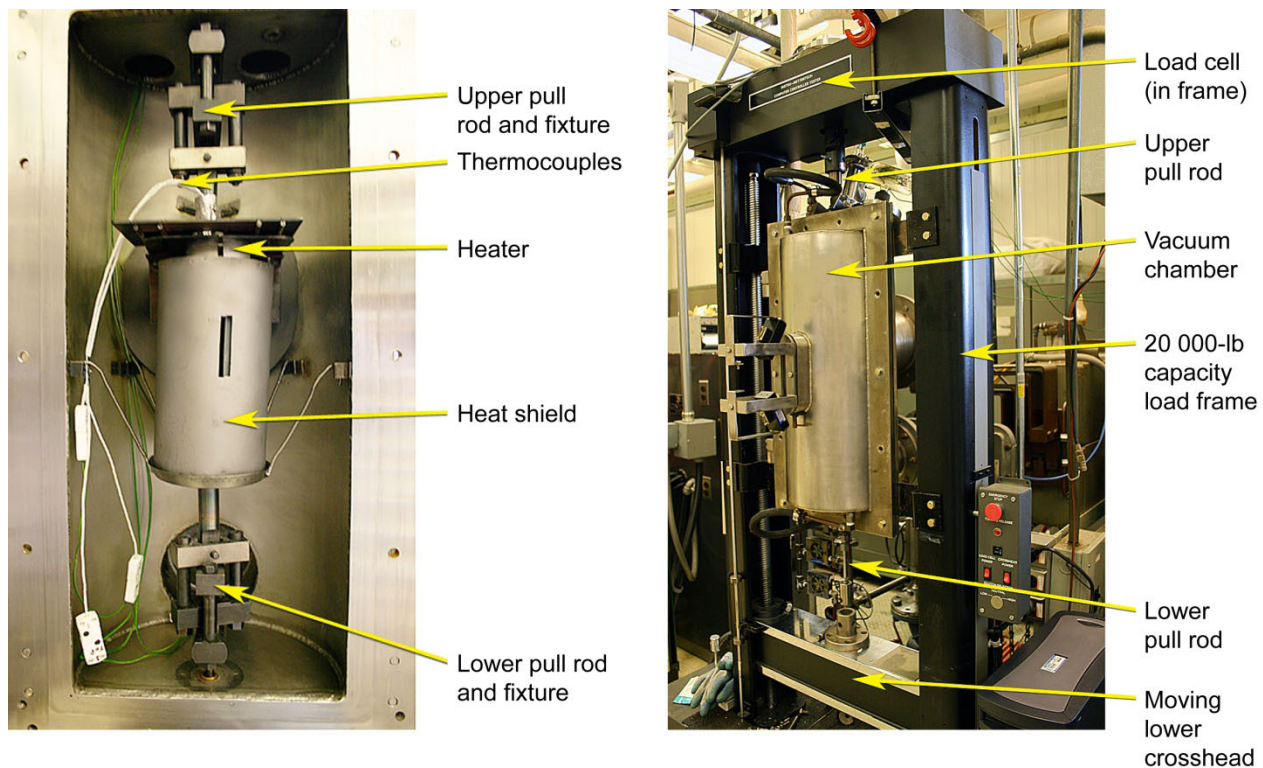


Figure 6.—Vacuum creep step-loading test frame (TM-4).

**Step-loading vacuum creep testing.**—An Instron TT series tensile test frame designated TM-4 (Fig. 6) was upgraded to computer data acquisition and control by the Instru-Met Corporation<sup>3</sup> using MTS Systems Corporation<sup>4</sup> TestWorks 4 testing software and associated MTS hardware. The software allows a load and recording displacement to be held over extended periods. The programming portion of the software allowed for developing a stepped sequence of loads and times. The sample was monitored continually, and data points were logged when the sample underwent a 0.01-percent change in strain. Each data point consisted of the elapsed time, load, and strain. The desired load was placed on the sample by moving the crosshead beneath the chamber downwards and pulling on the sample until the load cell measured the desired load. The movement of the crosshead was measured using an optical encoder to determine the displacement of the sample during creep.

One notable difference in the two types of load frames is that TM-4 uses a solid heater element rather than a mesh heater element. Temperature was controlled using a Type R thermocouple tied to the center of the specimen's gauge section. The over-temperature thermocouple was attached to the top of the specimen's gauge section, and a recording thermocouple was attached to the bottom of the specimen's gauge section. The gradient was not recorded, but general observations of the three temperature readouts indicated a temperature gradient of less than 5 °C (9 °F).

As with the LVR data for the constant-load tests, all displacement was assumed to occur in the reduced section of the specimens. Some creep occurs in the transition regions or sample shoulders, and that creep depends on the specimen geometry. If sufficiently large, the creep strain in the transition regions leads to an overestimate of the total creep since the total displacement divided by just the reduced gauge section length is used to calculate the creep strain.

<sup>3</sup>Instru-Met Corporation, 999 Rahway Avenue, Union, NJ 07083.

<sup>4</sup>MTS Systems Corporation, 14000 Technology Drive, Eden Prairie, MN 55344.

So that the error introduced by this assumption and the difference in specimen geometries could be estimated, the area of the sample for both specimen designs was calculated as a function of the distance along the long axis of the specimen. For this calculation, the zero point was assumed to be the transition from the straight uniform gauge section to the curved shoulder region. Only one-half of the specimen was considered since the samples were symmetric about the center point of the samples. The shoulders were a segment of a circle with the center at zero along the length of the sample and offset by the radius of the circle from the edge or surface of the uniform gauge section. This allowed the specimen shoulder width (flat-sheet specimens) or radius (round specimens) to be expressed as a function of the distance from the zero point. Knowing the thickness and width of the sheet specimens or the radius for the round specimens allowed the area of the specimen in the shoulder to be calculated as a function of distance along the long axis of the specimen.

Since the load was constant at all points in the specimen, the stress was calculated at each point in the transition region by dividing the applied load by the area of the cross section in the shoulders at that point. The creep rate for each point was estimated using the regression equation for the creep rate and the calculated stress at each point. The total displacement at each point was estimated by multiplying the creep rate by the specimen life. Summing the displacements at each point over the life of the test allowed the total strain in the transition region to be estimated.

Figure 7 shows the calculated total strains for tests conducted at 500 °C/100 MPa, 650 °C/50 MPa, and 800 °C/25 MPa (932 °F/14.5 ksi, 1202 °F/17.2 ksi, and 1472 °F/3.6 ksi). These stresses were selected because they were near the high end of the experimental values tested. A high value was desired since the stress decreases as the area increases and could easily drop below previously tested stress levels. The selected values allowed the rates to be calculated over the entire stress range experienced by the transition regions based on experimental data without the need to extrapolate except for the lowest stresses. The worst case as defined by the most creep strain, 650 °C/50 MPa, had a strain of  $1.02 \times 10^{-5}$  for the sheet specimen and  $3.56 \times 10^{-6}$  for the round specimen. The strain in both specimen geometries was miniscule in comparison to the typical total strains of 0.05 to 0.15 at failure observed by the LVR or optical encoder.

Because the frames measure displacement remote from the specimen, displacements also can be caused by creep of the fixtures, compliance of the machine, and other factors. Large-diameter, highly creep resistant materials were used for the fixtures. For the portion in the hot zone, no attempt was made to calculate the displacement from creep, since the area of the fixtures was at least 9 times greater than the maximum area of the test specimens and their creep rates were much lower at the test temperatures. On the basis of the low strain for the GRCop-84 in the transition regions and much lower creep rates for the fixture materials, it was assumed that the creep in the fixtures was nil.

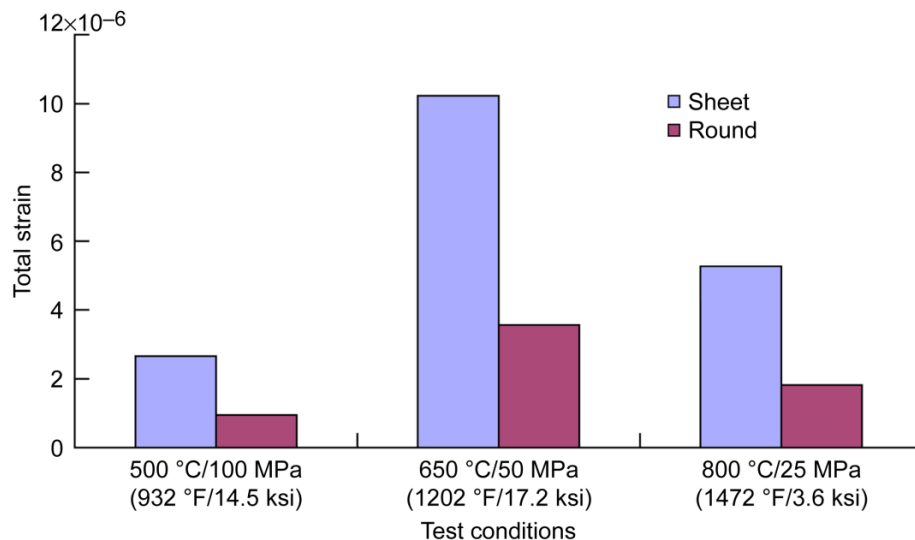


Figure 7.—Total strain in specimen transition region.

It is difficult to measure compliance of the machine without an extensometer or other direct measurement of the specimen strain, but the low loads ( $\ll 4.4$  kN) on a 44.5-kN- (10 000-lb<sub>f</sub>-) capacity frame probably mean that the contribution from the compliance of the machine is minimal as well. In addition, the 0.2-percent-offset yield strength of GRCop-84 is low at the test temperatures (Ref. 4), and the onset of plastic deformation occurs at even lower stresses (as shown in the stress-strain curves in Ref. 4), so specimens tend to yield plastically rather than stretch elastically. The low loads and plastic deformation make the error from machine compliance small and probably unobservable.

The only other known source of error in the displacement measurements is the slack in the load train, which leads to an initial large displacement upon loading. All subsequent strains have this initial strain incorporated into the measurement. Since that unknown initial strain value is constant for all subsequent displacement measurements, subtracting one measurement from another gives an accurate displacement between the two data points. If this difference is divided by the time between the two measurements, the creep rate can be accurately calculated in a manner similar to the calculation of creep rates for the Brew frames using the LVR data points.

So although two different load frames were used to test two different specimen geometries, the differences in the remotely measured displacements, and hence the strains used to calculate the creep rates, should not affect the results.

Step-loading vacuum creep testing was conducted to independently determine creep rate for comparison with the Brew frame data sets and to provide a calibrated standard for the creep test results. Varying the temperatures from test to test over a narrow range allowed for estimation of the deviation of the Brew frame sample temperature from the setpoint since the observed creep rate at a given load could be compared with the measured creep rate at various temperatures for that load. It also allowed for a better examination of the load and temperature sensitivity of GRCop-84 creep.

A series of tests were conducted at temperatures of 500, 525, 550, 650, 675, and 700 °C (932, 977, 1022, 1202, 1247, and 1292 °F) for specimens taken from sheet 3A1B. Table VII presents the load and hold times used.

TABLE VII.—STEP-LOADING CREEP RATE TEST PARAMETERS

Step	Applied stress, MPa	Time, h	Step	Applied stress, MPa	Time, h	Step	Applied stress, MPa	Time, h
500 °C (932 °F)			525 °C (977 °F)			550 °C (1022 °F)		
1	70.0	5	1	70.0	5	1	70.0	5
2	73.0	5	2	73.0	5	2	73.0	5
3	76.0	5	3	76.0	5	3	76.0	5
4	79.0	5	4	79.0	5	4	79.0	5
5	82.0	5	5	82.0	5	5	82.0	5
6	85.0	3	6	85.0	3	6	85.0	3
7	88.0	3	7	88.0	3	7	88.0	3
8	91.0	3	8	91.0	3	8	91.0	3
9	94.0	3	9	94.0	3	9	94.0	3
10	97.0	3	10	97.0	3	10	97.0	3
11	100.0	2	11	100.0	2	11	100.0	2
12	103.0	2	12	103.0	2	12	103.0	2
13	106.0	2	13	106.0	2	13	106.0	2
14	109.0	2	14	109.0	2	14	109.0	2
15	112.0	2	15	112.0	2	15	112.0	2
16	115.0	1	16	115.0	1	16	115.0	1
17	118.0	1	17	118.0	1	17	118.0	1
18	121.0	1	18	121.0	1	18	121.0	1
19	124.0	1	19	124.0	1	19	124.0	1
20	127.0	1	20	127.0	1	20	127.0	1

TABLE VII.—Concluded.

Step	Applied stress, MPa	Time, h	Step	Applied stress, MPa	Time, h	Step	Applied stress, MPa	Time, h
650 °C (1202 °F)			675 °C (1247 °F)			700 °C (1292 °F)		
1	27.5	5	1	27.5	5	1	27.5	5
2	30.0	5	2	30.0	3	2	30.0	3
3	32.5	5	3	32.5	2	3	32.5	2
4	35.0	5	4	35.0	1	4	35.0	1
5	37.5	5	5	37.5	1	5	37.5	1
6	40.0	3	6	40.0	1	6	40.0	1
7	42.5	3	7	42.5	.5	7	42.5	.5
8	45.0	3	8	45.0	.5	8	45.0	.5
9	47.5	3	9	47.5	.5	9	47.5	.5
10	50.0	3	10	50.0	.5	10	50.0	.5
11	52.5	2	11	52.5	.2	11	52.5	.2
12	55.0	2	12	55.0	.2	12	55.0	.2
13	57.5	2	13	57.5	.2	13	57.5	.2
14	60.0	2	14	60.0	.2	14	60.0	.2
15	62.5	2	15	62.5	.2	15	62.5	.2
16	65.0	1	16	65.0	.2	16	65.0	.2
17	67.5	1	17	67.5	.2	17	67.5	.2
18	70.0	1	18	70.0	.2	18	70.0	.2
19	72.5	14	19	72.5	.2	19	72.5	.2
20	75.0	1	20	75.0	.2	20	75.0	.2

## Results and Discussion

This work was conducted in three sequential stages. During stage I, an initial survey was conducted to determine if data were identical among Brew frames. Stage II postulated various root causes, examined and identified the main sources of variation, and independently determined creep rate through step loading. In stage III, the final stage, tests were conducted to validate that each Brew frame provided similar results and to determine if the anticipated effects of processing could be discerned. The results of each stage are presented and discussed separately since each stage builds on the preceding stage.

### Stage I—Initial Survey

The initial survey compared creep response as a function of Brew frame at a constant stress (105 MPa) and temperature (500 °C) for material from sheet 3HCS. Table VIII shows the results. The steady-state creep rate was determined using the slope of the linear portion of the creep curve that had the minimum slope.

On the basis of the Monkman-Grant relationship (Ref. 8), the data plotted as  $\log_{10}(\text{creep life})$ , with the life in seconds, versus  $\log_{10}(\text{creep rate})$ , with the rate in reciprocal seconds, should produce a straight line. Figure 8 shows that the data set follows the Monkman-Grant relationship well. The Monkman-Grant model was used to check the data for outliers since it is independent of stress and temperature—the two independent variables typically most influential in creep testing. A least-squares linear regression with a two-way 95-percent confidence interval was conducted to determine the power law equation for the observed relationship. The fit of the data indicates that there are no apparent outliers. Therefore, all the tests were considered to be valid.

TABLE VIII.—CREEP BEHAVIOR AS A FUNCTION OF BREW FRAME  
 [Stress, 105.0 MPa; setpoint temperature, 500 °C.]

Test	Brew frame	Specimen number of sample 3HCS	Steady-state creep rate, s <sup>-1</sup>	Creep life, h	Total strain, percent
2A	1	22T	1.32×10 <sup>-5</sup>	2.7	18.6
3A	1	4T	8.11×10 <sup>-6</sup>	4.6	21.5
1A	1	20L	5.71×10 <sup>-6</sup>	5.6	22.8
6A	2	1T	1.52×10 <sup>-4</sup>	.4	37.4
4A	2	25L	8.08×10 <sup>-5</sup>	.6	28.7
5A	2	13T	7.99×10 <sup>-5</sup>	.6	33.9
7A	3	15L	4.36×10 <sup>-5</sup>	1.0	22.1
9A	3	26L	3.56×10 <sup>-5</sup>	1.1	18.3
8A	3	1L	1.80×10 <sup>-5</sup>	2.2	25.8
11A	4	14L	3.14×10 <sup>-5</sup>	1.2	27.4
10A	4	15T	2.98×10 <sup>-5</sup>	1.4	32.0
1	4	24T	2.39×10 <sup>-5</sup>	1.5	23.6
12A	4	20T	2.67×10 <sup>-5</sup>	1.5	31.8
2	4	22L	1.76×10 <sup>-5</sup>	1.9	25.3
14A	5	18L	6.81×10 <sup>-6</sup>	4.7	33.1
13A	5	17L	2.27×10 <sup>-7</sup>	69.5	33.6
<sup>a</sup> 15A	5	7L	1.82×10 <sup>-8</sup>	330.6	20.7

<sup>a</sup>Sample 15A–7L did not break, but the test was stopped after 330.6 h.

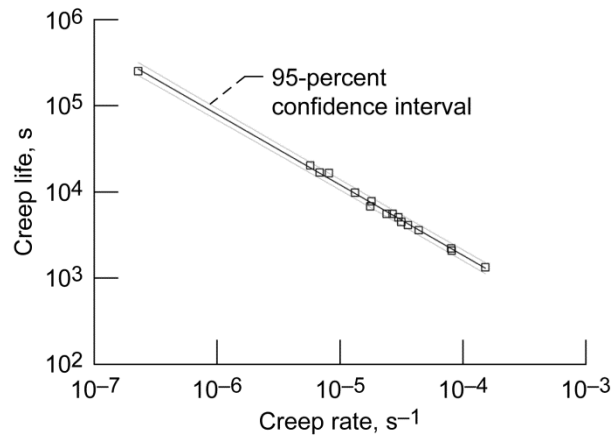


Figure 8.—Creep life versus creep rate (life =  $9.09 \times 10^{-3}$  (rate)<sup>-0.82</sup>) for stage 1 creep tests. Coefficient of determination,  $R^2 = 0.9975$ .

However, when creep life at 500 °C/105 MPa was plotted by Brew frame, as shown in Figure 9, each frame had a different mean creep life. If test conditions had been identical, the lives should have been similar with a small standard deviation for the  $\log_{10}(\text{creep life})$  values. The absolute range for each Brew frame on a logarithmic scale was similar among the frames. The single exception was for Brew frame 5, which had one test that did not fail after 330.6 h, the time when the test was terminated. Figure 10 shows creep curves for all the tests conducted at 500 °C/105 MPa. The variability in the shapes and magnitudes of the curves confirms that each Brew frame had a very different response. This indicates that the test conditions were not identical as assumed.

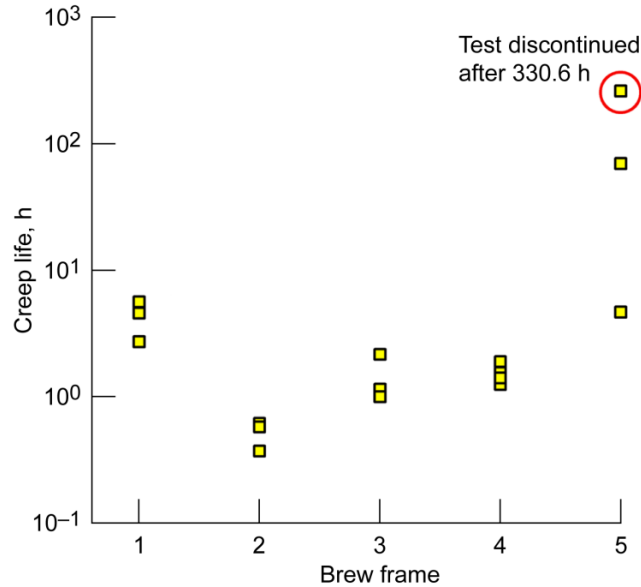


Figure 9.—Creep life as a function of Brew frame for GRCop-84 tested at 500 °C/105 MPa.

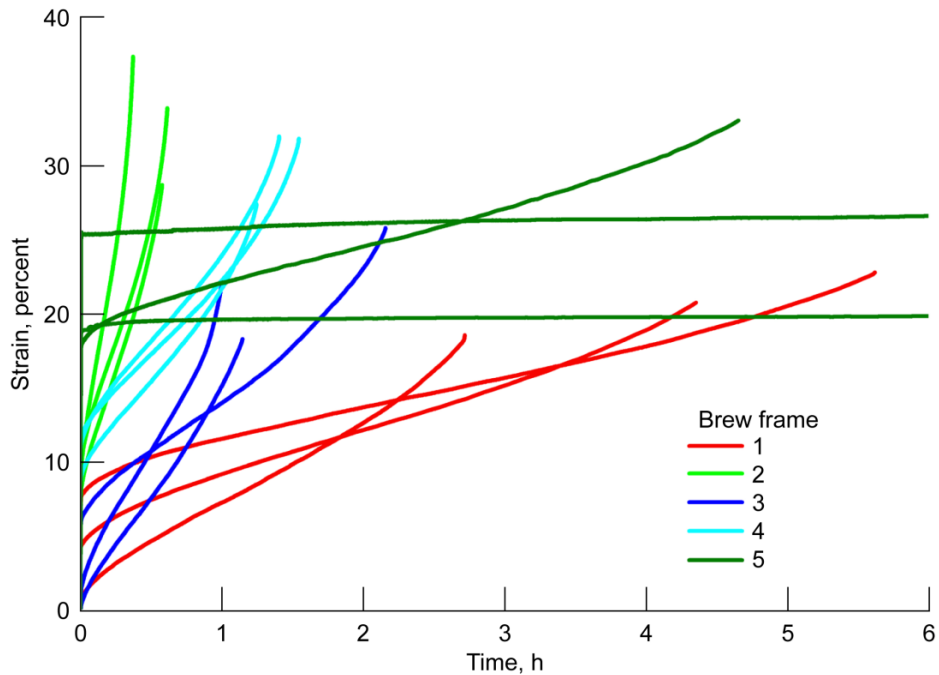


Figure 10.—Comparison of creep rate curves as a function of Brew frame for GRCop-84 with the same process history tested at 500 °C/105 MPa.

A one-way ANOVA was conducted on the life data using  $\log_{10}(\text{creep life})$  as the dependent variable to confirm that there was a statistical difference in the means of the five Brew frames as suspected. Table IX shows the results. An SNK test was used to compare the means. As expected, Brew frame 5 had a much different mean, but there were also statistical differences detected between Brew frame 1 and Brew frames 2, 3, and 4. Brew frames 2, 3, and 4 gave statistically equal results.

This result for identical test conditions of specimens with the same process history was not expected. It was reasoned that whatever was causing this difference was responsible for much of the variation seen in the data shown in Figures 1 and 2. Since the specimen material is assumed to have been identical, each Brew frame should have had a similar creep curve, creep rate, and creep life for a given temperature and creep stress. For the secondary, or steady-state, slope to change significantly, either temperature or stress would need to be different among these tests. Figure 11 illustrates how the creep response would change with increasing temperature or stress (Ref. 9).

These results clearly demonstrate the need for additional testing to determine the source of variation and to develop corrective actions to improve the creep tests.

TABLE IX.—RESULTS OF ONE-WAY ANALYSIS OF VARIANCE (ANOVA) FOR CREEP LIVES

Source of variation	Degrees of freedom	Sum of squares	Mean squares	F value <sup>a</sup>	Probability
Between subjects	2	0.122	0.0610	-----	-----
Between treatments	4	3.062	.765	7.463	0.011
Residual	7	.718	.103	-----	-----
Total	13	4.119	.317	-----	-----

<sup>a</sup>The value of the F distribution for X degrees of freedom associated with the numerator and Y degrees of freedom associated with the denominator.

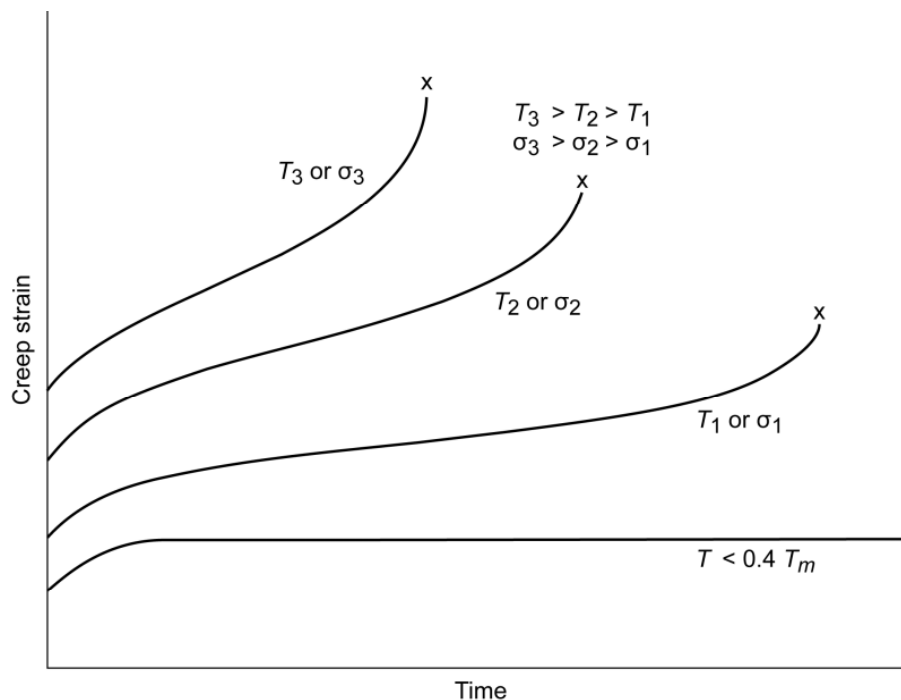


Figure 11.—Typical creep curves as temperature,  $T$ , or initial applied stress,  $\sigma$ , is changed (Ref. 9)  $T_m$ , melting temperature.

## Stage II—Identifying Sources of Variation

**Constant-load vacuum creep testing.**—Investigations of various root causes that could produce different creep responses were conducted. Although these were centered on temperature and load, other test aspects were also considered. A detailed review of the creep test procedure, thermocouple and instrumentation calibration, friction in the mechanical feedthrough ball joint, and resistance from the weight of the rubber cooling hose hanging on the upper mechanical feedthrough ball joint were examined qualitatively and, when possible, quantitatively. They were found not to be detectably different among test frames on the basis of a review of the calibration data sheets, calibrated simulated input data, measured loads, and when quantitative measurements were not possible, optical and physical examination of the frames. Minor changes, such as supporting the hoses closer to the upper pull rod, produced no detectable changes in loads or temperatures.

Operator error was assumed to be random, but some systematic factors could have been introduced through an operator bias. A systematic error would result in a shift of the creep life to a higher or lower value, but it should have been relatively uniform and not have affected the scatter in the data set. Differences between various operators were recognized as a potential source of error and scatter. Only one operator was used in this study to remove operator-to-operator variability from the possible sources of errors.

The measurement technique for the displacements was also examined. Measuring the displacement by measuring the travel of the load train introduces a random variability from equipment measurement errors. There is also a systematic error because the total displacement includes deformation outside of the gauge section. However, as was pointed out in the Experimental Procedure section, these displacements are miniscule in comparison to the displacements from creep. The errors in measurement would tend to be small, a few percent or less of the value, and would only affect the creep rates, not the creep lives. Since the creep rates and the creep lives had similar variability, the contribution of this assumption was shown to be small relative to the observed variability. As such, the measurement of the displacements remotely was not considered to be a primary source of variability.

It was determined that, to examine temperature and load differences, additional instrumentation would be needed. On Brew frames 3 and 4, provisions were made to install thermocouples to monitor the specimen temperature, and a load cell was placed in the lower pull rod. In addition, provisions were made to pressurize the chamber of Brew frame 3 with helium at slightly less than 1 atm in an attempt to try to improve the heat transfer rate and uniformity from the heater to the sample. These frames then served as prototypes for potential equipment upgrades to the load frames. A series of tests to examine the variability in loads and temperatures were conducted at various temperatures and loads following the same setup and test procedures for each test. Table X shows the test conditions and results.

Test 1 was conducted on Brew frame 3 with a temperature setpoint of 500 °C (932 °F) and an initial stress of 105 MPa (15.2 ksi). The load was monitored periodically and was a constant value throughout the test. The load was compared with the balance pan weight and differed slightly, which was attributed to errors arising from zeroing the electronics, friction in the load train, and the inherent error of the load cell based on the load cell specifications. Because the load did not vary during the test and the small load differences would not explain the different shaped creep curves, the main emphasis shifted to temperature differences. The subsequent creep tests confirmed the accuracy, reproducibility, and stability of the loads.

During test 1, the specimen temperature was found to be 43 °C (77 °F) higher than the controller setpoint, and from top to bottom along the sample, a temperature gradient of 44 °C (79 °F) was observed. Such a large temperature difference and gradient would have a profound effect on the creep properties, and they could produce great variability if either varied from test to test or from frame to frame while the setpoint remained the same. However, if the temperature difference and the thermal gradient were both consistent for all tests, they would not produce variability in the creep responses. Instead, they would introduce a systematic error into the creep testing. The creep rate would be higher and the creep life shorter than for a sample tested at the proper, lower sample temperature.

TABLE X.—GRCop-84 SHEET SPECIMEN TEST CONDITIONS AND RESULTS  
USED FOR IDENTIFYING SOURCES OF VARIATION

(a) Test comments.

Test	
1	First run with top, middle, and bottom thermocouple; control thermocouple might be as much as 1/8 to 1/4 in. away from sample
2	Control thermocouple located 1/16 in. away from specimen center; grips not symmetrical
3	Control thermocouple located 1/16 in. away from specimen center; grips not symmetrical and different from Brew frame 3 combination
4	Control thermocouple located 1/16 in. away from specimen center; grips not symmetrical
5	Control thermocouple located 1/16 in. away from specimen center; grips not symmetrical and different from Brew frame 3 combination
6	Control thermocouple located 1/16 in. away from specimen center; grips not symmetrical
7	Control thermocouple located 1/16 in. away from specimen center; grips not symmetrical and different from Brew frame 3 combination
8	Symmetrical grips and control thermocouple 1/16 in. away from specimen center
9	Symmetrical grips and control thermocouple 1/16 in. away from specimen center
10	Helium atmosphere
11	Helium atmosphere
12	Helium atmosphere
13	Helium atmosphere
14	Helium atmosphere
15	Helium atmosphere

(b) Conditions and results.

Test	Brew frame	Specimen		Applied stress, MPa	Set-point temp., °C	Average temperature of various thermocouples, °C			Temperature difference between thermocouples, °C		Life, h	Creep rate, s <sup>-1</sup>	
						Top	Middle	Bottom	Bottom to top	Bottom to control			
1	3	12	1a5c-350	105	500	499.3	537.0	542.9	43.6	42.9	2.30	1.22×10 <sup>-5</sup>	
2	3	15	1a5c-450	105	500	499.2	523.7	532.8	33.6	32.8	1.62	1.99×10 <sup>-6</sup>	
3	4	18	1a3b-450	105	500	499.1	504.1	511.0	11.9	11.0	1.85	1.55×10 <sup>-6</sup>	
4	3	16	1a3c-450	17	800	800.0	805.2	812.0	12.0	12.0	24.62	2.31×10 <sup>-7</sup>	
5	4	17	1a5c-450	17	800	799.4	826.1	832.1	32.8	32.1	5.04	7.18×10 <sup>-6</sup>	
6	3	24	1a3b-450	44.3	650	649.9	658.8	668.1	18.2	18.1	4.98	3.82×10 <sup>-6</sup>	
7	4	22	1a5c-350	44.3	650	649.5	674.9	682.1	32.6	32.1	8.78	1.53×10 <sup>-6</sup>	
8	3	14	1a3c-450	105	500	499.6	529.2	534.1	34.5	34.1	4.82	6.54×10 <sup>-6</sup>	
9	4	21	1a5c-350	105	500	499.2	524.3	537.0	37.8	37.0	6.18	4.08×10 <sup>-6</sup>	
10	3	20	DLE4a2	105	500	499.2	500.6	506.6	7.3	6.6	4.57	6.34×10 <sup>-6</sup>	
11	3	21	DLE4a2	105	500	499.0	496.9	504.7	5.7	4.7	6.74	5.79×10 <sup>-6</sup>	
12	3	22	DLE4a2	44.3	650	649.4	643.7	653.4	4.1	3.4	3.11	3.93×10 <sup>-6</sup>	
13	3	23	DLE4a2	44.3	650	649.4	643.1	651.8	2.3	1.8	3.68	3.19×10 <sup>-6</sup>	
14	3	24	DLE4a2	17	800	Specimen broke on loading							
15	3	25	DLE4a2	17	800	800.1	794.0	801.6	1.5	1.6	5.35	1.96×10 <sup>-6</sup>	

Possible reasons for the large temperature differences between the control and specimen were investigated first. It was identified that the control thermocouple was not being located precisely relative to the specimen. The farther the control thermocouple was from the specimen, the greater the temperature difference was between the control thermocouple and the specimen. Ideally, the control thermocouple should touch the specimen, but this is not suitable for these tests because a bending moment would be introduced. The closest practical control thermocouple position was 1.57 mm (0.062 in.) away from the specimen when the specimen was at room temperature. A 1.57-mm feeler gauge was fabricated to aid in consistent positioning, and the test procedure was modified to include positioning the chamber thermocouple with the feeler gauge. All subsequent tests were run with the control thermocouple at this standoff distance.

Test 2 was again conducted on Brew frame 3 using a 500 °C (932 °F) setpoint and a 105-MPa (15.2-ksi) initial stress. The control thermocouple standoff was set using the new thermocouple positioning technique. The specimen temperature was 33 °C (59 °F) higher than the controller setpoint, and the temperature gradient along the specimen was 34 °C (61 °F). This was a slight improvement over the first test, but it also highlighted the potential variability of both the temperature difference and the thermal gradient with even small changes in control thermocouple position.

Test 3 was conducted on Brew frame 4 still using a control thermocouple setpoint of 500 °C (932 °F) and an initial stress of 105 MPa (15.2 ksi). The same feeler gauge used for the Brew frame 3 test was used to position the control thermocouple. The specimen temperature was 11 °C (20 °F) higher than the controller setpoint, and the temperature gradient along the specimen was 12 °C (22 °F). This showed that even when the same gap was used there were large differences in the specimen temperature and gradient from load frame to load frame.

Tests 4 and 5 were conducted using a control thermocouple setpoint of 800 °C (1472 °F) and an initial stress of 17 MPa (2.5 ksi) employing Brew frames 3 and 4, respectively. The higher temperature was expected to improve radiative heat transfer and to minimize temperature differences and gradients. For Brew frame 3, the specimen temperature was 12 °C (22 °F) higher than the controller setpoint, and the temperature gradient along the specimen was 12 °C (22 °F). For Brew frame 4, the specimen temperature was 32 °C (58 °F) higher than the controller setpoint, and the temperature gradient along the specimen was 33 °C (59 °F). These differences and gradients had Brew frame 4 now being hotter with a larger gradient than Brew frame 3. This is the opposite of the results obtained in tests 2 and 3. This highlighted the frame-to-frame and specimen-to-specimen variability in temperature that can contribute to the variability in creep rate and creep life.

Tests 6 and 7 were conducted using a control thermocouple setpoint of 650 °C (1202 °F) and an initial applied stress of 44.3 MPa (6.4 ksi) employing Brew frames 3 and 4, respectively. For Brew frame 3, the specimen temperature was 18 °C (32 °F) higher than the controller setpoint, and the temperature gradient along the specimen was 18 °C (32 °F). For Brew frame 4, the specimen temperature was 32 °C (58 °F) higher than the controller setpoint, and the temperature gradient along the specimen was 33 °C (59 °F).

From these seven tests, it was observed that the specimen temperature and temperature gradients were different between Brew frames 3 and 4 despite the consistent location of the control thermocouple. In both Brew frames, the specimen temperature was consistently hotter than the setpoint control temperature, and the temperature gradient along the length of the specimen from top to bottom was consistently hottest at the bottom of the gauge length and coldest at the top. The top thermocouple most closely matched the control thermocouple. The differences and the gradients were also noted to vary even within a single Brew frame.

It was observed that the specimen grip fixtures were not fully symmetrical and that the tooling arrangement was different between Brew frames 3 and 4. It was reasoned that the different mass of the grips that are attached to the water-cooled pull rods transferred heat unevenly away from the specimen and affected the specimen temperature distribution. Similarly, the different tooling arrangement between Brew frames 3 and 4 would produce different temperature distributions between the frames. Sufficient 310 stainless steel tooling was fabricated using the same designs so that the top and bottom tooling would be identical in all of the Brew frames to eliminate this potential source of variation.

Tests 8 and 9 were conducted using symmetrical grips, again using a control thermocouple setpoint of 500 °C (932 °F) and an initial stress of 105 MPa (15.2 ksi) employing Brew frames 3 and 4, respectively. The specimen temperature gradients were now similar for both Brew frames. For Brew frame 3, the specimen temperature was 34 °C (61 °F) higher than the controller setpoint, and the temperature gradient along the specimen was 35 °C (63 °F). For Brew frame 4, the specimen temperature was 37 °C (67 °F) higher than the controller setpoint, and the temperature gradient along the specimen was 38 °C (68 °F).

On the basis of these results, which indicate that grip material and geometry can affect the specimen gradients, the testing procedure was updated to require symmetrical fixturing made from the same material. This change was implemented for all subsequent testing. Through trial and error it may be possible to use asymmetrical grips to reduce the gradient, but the potential improvement was not addressed in this study because of limited time and resources. In addition, asymmetrical grips were not considered to be suitable for standard testing given the wide range of materials tested in the laboratory, their greatly varying test temperatures, and the normally low volume of samples.

The heaters were also examined. The bottom of each heater had a solid band rather than a mesh (see Fig. 6(b)). The top also had a band, but it was split and attached to water-cooled Cu electrical power supplies that would tend to cool the top. The authors believe that the solid band on the heater base provided a higher heat flux to the sample and pull rods than the open mesh provided. The upper section was in contact with the water-cooled electrical feedthroughs, which may have reduced its heat flux as well. The solid heater used for the step-loading calibration runs had a thermal gradient typically less than 5 °C (9 °F) as measured by the three attached thermocouples. This improvement, while using very similar geometries for the heaters, indicates that the design of the heater is important.

The mesh heaters also tended to bow and otherwise deform more than the solid heater. This variability of the gap between the sample and the heater introduced some variability into the temperature and specimen temperature gradients as well. Solid heaters with a more consistent geometry from heater to heater that retain that geometry from specimen to specimen could help to reduce the observed variability.

Replicate tests were not conducted because of equipment schedule constraints, but the specimen temperature gradients were now similar for both Brew frames and were believed to be reproducible. Although the thermal gradients were larger than desired, the consistency of the gradients means that they will not contribute to the variability in the creep rates and lives. Additional work is planned to determine if the gradients can be reduced through improved heater design and if the applicable ASTM International standards for temperature gradients in creep tests can be met.

Tests 10 to 15 were conducted in Brew frame 3 with a helium atmosphere and symmetrical grips. Duplicate tests were performed with the control thermocouple setpoint and pressure at 500 °C/105 MPa, 650 °C/44.3 MPa, and 800 °C/17 MPa (932 °F/15.2 ksi, 1202 °F/6.4 ksi, and 1472 °F/2.5 ksi). No corrections were made to match the specimen temperatures to the setpoint temperatures.

When helium was used, the average specimen temperature for all of these conditions was 4 °C (7 °F) higher than the controller setpoint. The temperature gradient along the specimen was reduced to 4 °C (7 °F). The helium clearly improved the specimen temperature uniformity and more closely matched the sample temperature to the control thermocouple temperature.

Although the life and creep results do not lend themselves well to statistical analysis because there are no true repeats, general observations can be made regarding the differences in what should be identical tests. The creep rates and lives for the 500 °C/105 MPa and 800 °C/17 MPa tests with fairly large temperature differences and gradients varied by almost 1 order of magnitude, and the creep life varied by about the same amount. Even the 650 °C/44.3 MPa data set, with its more consistent temperatures and gradients, shows a 1/2 order of magnitude variability. In contrast, the subset of tests conducted in a helium atmosphere with small temperature gradients and differences had reproducible creep rates and creep lives. This underscores the effect of temperature on the variability of creep properties.

**Step-loading vacuum creep testing.**—Concurrent with the constant-load creep testing, step-loading vacuum creep testing was conducted to independently determine creep rate as a way to establish a standard for the constant-load tests. The variations in temperature and stress investigated would also assist in quantifying the sensitivity of GRCop-84 to small changes in temperature and stress.

A limited series of tests were conducted at the temperatures and loads listed in Table VII using sheet specimens from the same source as the Brew frame creep test specimens. During these tests, the combination of loads and hold times generated failure of the samples in all cases before the entire series of 20 steps were completed. This did not affect the validity of the tests or the results, but it did result in a smaller data set for each test.

The results of the step-loading creep tests are presented in Table XI and plotted in Figure 12. A least-squares-fit power law regression was used to estimate the creep rate versus stress. The general form of the equation used is

$$\dot{\epsilon} = A \sigma^n \quad (3)$$

where  $\dot{\epsilon}$  is creep rate in reciprocal seconds,  $A$  is a constant,  $\sigma$  is load (in MPa), and  $n$  is the stress exponent. Table XII presents values for  $A$  and  $n$ . Included for comparison are the results for an as-extruded GRCop-84 bar and an annealed 6.5-mm (0.255-in.) GRCop-84 plate from other creep testing during this program (Refs. 2 and 10). The results for  $n$  indicate that power law creep predominated as expected.

Several important points are illustrated in Figure 12. First, the creep rate is highly sensitive to temperature. A 50 °C (90 °F) temperature increase results in a 1 order of magnitude increase in the steady-state creep rate.

TABLE XI.—STEP-LOADING CREEP TEST RESULTS FOR VARIOUS TEMPERATURES

Step	Stress, MPa	Creep rate, s <sup>-1</sup>	Step	Stress, MPa	Creep rate, s <sup>-1</sup>	Step	Stress, MPa	Creep rate, s <sup>-1</sup>
500 °C (932 °F)			525 °C (977 °F)			550 °C (1022 °F)		
1	70.0	3.2×10 <sup>-7</sup>	1	70.0	5.8×10 <sup>-7</sup>	1	69.9	2.3×10 <sup>-6</sup>
2	73.0	3.0×10 <sup>-7</sup>	2	73.0	4.5×10 <sup>-7</sup>	2	72.9	3.3×10 <sup>-6</sup>
3	76.0	3.0×10 <sup>-7</sup>	3	75.9	4.9×10 <sup>-7</sup>	3	75.9	5.6×10 <sup>-6</sup>
4	79.0	3.5×10 <sup>-7</sup>	4	78.9	5.8×10 <sup>-7</sup>	700 °C (1292 °F)		
5	82.0	4.2×10 <sup>-7</sup>	5	81.9	9.7×10 <sup>-7</sup>	1	27.5	1.4×10 <sup>-6</sup>
6	85.0	4.7×10 <sup>-7</sup>	6	84.9	1.4×10 <sup>-6</sup>	2	30.0	2.1×10 <sup>-6</sup>
7	88.0	5.9×10 <sup>-7</sup>	7	87.9	2.2×10 <sup>-6</sup>	3	32.5	4.1×10 <sup>-6</sup>
8	91.0	7.6×10 <sup>-7</sup>	675 °C (1247 °F)			4	35.0	9.8×10 <sup>-6</sup>
9	93.9	9.8×10 <sup>-7</sup>	1	27.4	9.5×10 <sup>-7</sup>			
10	96.9	1.3×10 <sup>-6</sup>	2	29.9	1.0×10 <sup>-6</sup>			
11	99.9	1.9×10 <sup>-6</sup>	3	32.3	1.5×10 <sup>-6</sup>			
12	102.9	3.0×10 <sup>-6</sup>	4	34.8	2.9×10 <sup>-6</sup>			
650 °C (1202 °F)			5	37.3	4.5×10 <sup>-6</sup>			
1	27.5	3.4×10 <sup>-7</sup>	6	39.8	8.1×10 <sup>-6</sup>			
2	30.0	4.1×10 <sup>-7</sup>	7	42.1	1.7×10 <sup>-5</sup>			
3	32.5	4.3×10 <sup>-7</sup>						
4	35.0	6.3×10 <sup>-7</sup>						
5	37.5	9.5×10 <sup>-7</sup>						
6	37.5	1.6×10 <sup>-6</sup>						
7	42.5	3.0×10 <sup>-6</sup>						

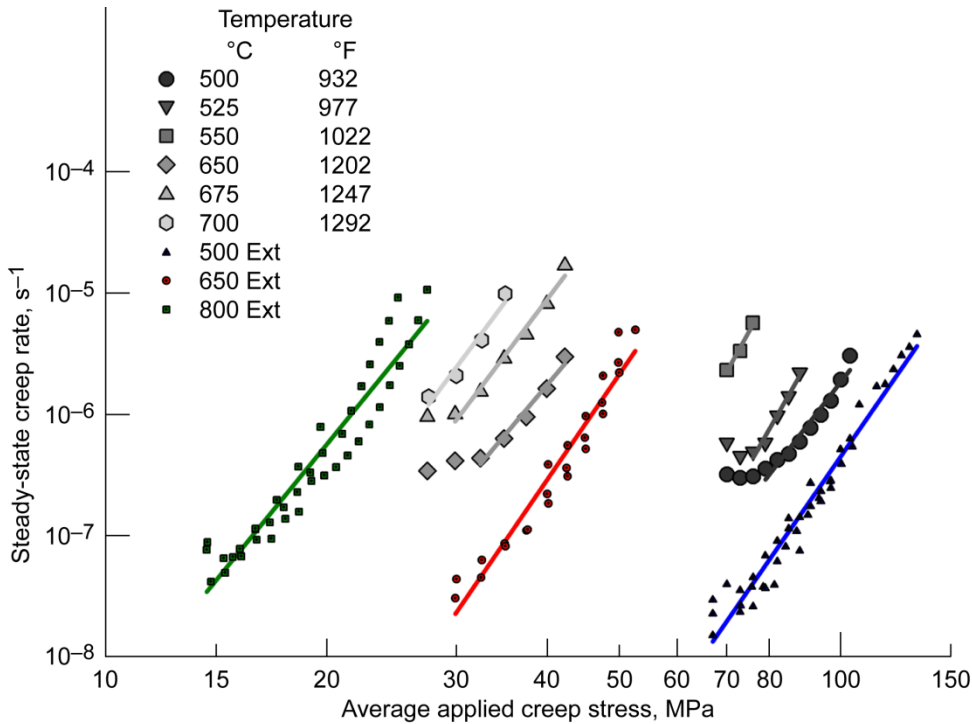


Figure 12.—Creep rate determined by step loading.

TABLE XII.—REGRESSION COEFFICIENTS AND GOODNESS OF FIT

Creep test temperature		Sample type	Equation coefficients, <sup>a</sup>		$R^2$
°C	°F		$\dot{\epsilon} = A \sigma^n$		
			$A$	$n$	
500	932	Rolled 1.1-mm sheet 3A1B ↓	$8.06 \times 10^{-22}$	7.66	0.89
525	977		$5.35 \times 10^{-27}$	10.59	.98
550	1022		$2.21 \times 10^{-26}$	10.85	.99
650	1202		$1.36 \times 10^{-14}$	5.05	.87
675	1247		$1.09 \times 10^{-16}$	6.80	.94
700	1292		$2.57 \times 10^{-18}$	8.11	.96
Prior testing					
500	932	Extruded 25-mm bar	$7.48 \times 10^{-32}$	12.10	0.98
500	932	Rolled 6.5-mm plate	$1.25 \times 10^{-24}$	8.78	.96
650	1202	Rolled 6.5-mm plate	$1.93 \times 10^{-21}$	8.86	.94
800	1472	Rolled 6.5-mm plate	$1.15 \times 10^{-16}$	7.45	.91

<sup>a</sup>  $\dot{\epsilon}$ , creep rate;  $A$ , constant;  $\sigma$ , load;  $n$ , stress exponent;  $R^2$ , simple coefficient of determination.

The creep rate is less sensitive to stress. A 10-MPa (1.4-ksi) change in stress would result in about 1/10 order of magnitude change in steady-state creep rate. Generally, the load is controllable to less than 4.4 N (1 lb<sub>f</sub>) using the dead weights. Although the variability in stress depends on specimen cross section, the variability in stress is normally 0.1 MPa (0.01 ksi) or less. Results of the sensitivity analysis indicate that this uncertainty in stress should not produce observable variability.

These results indicate that GRCop-84 creep behavior is more sensitive to small temperature changes than was previously appreciated. It also demonstrates that temperature is more likely than stress to be the source of the observed variability.

### Stage III—Verification

**GRCop-84 sheet.**—The preceding findings show that the specimen could be much hotter than the control thermocouple and that GRCop-84 creep behavior is more temperature sensitive than expected. We concluded that thermocouples had to be tied directly to the specimens in such a way that the beads were in intimate contact with the specimen to minimize the difference between the temperature controller setpoint temperature and the specimen temperature. The attachment also had to be done without having the thermocouples introduce a bending moment or other spurious stresses in the specimens.

A design using thermocouples with small alumina beads introduced from the bottom of the chamber was selected. Stainless steel wire was used to tie the thermocouples to the lower pull rod and the sample. As shown in Figure 6(c), the beads were in intimate physical contact with the sample. The flexible nature of the thermocouples minimized bending moments. The weight of the thermocouples was almost entirely supported by tying them to the lower pull rod to minimize any contribution that they may have had to the loads on the sample. Vacuum thermocouple feedthroughs were added to an existing port, and the three thermocouples were tied into the data acquisition system for recording.

Modifications to add thermocouples that could be tied directly to the specimens for each Brew frame were expected to permit more accurate and consistent specimen temperature control from test to test and from frame to frame. Therefore, a series of tests in vacuum and helium were conducted to demonstrate the improvements and to determine if the variations observed between Brew frames had been eliminated. Table XIII presents the results.

The vacuum and helium test creep life data for all test conditions were plotted against creep rate on a log-log scale and are shown in Figure 13. The Monkman-Grant relationship was again used to determine if there were any obvious outliers. Also included are data from stage I of the creep testing (original procedure) for comparison. Again, the new data fall on a straight line, indicating that there are no outliers. The least-squares fit for the power law equation is also nearly identical to the prior results, indicating that the changes in test methods and procedures did not change the creep behavior of GRCop-84.

Figure 14 shows the creep life data from the vacuum and helium tests plotted as a function of Brew frame for each test temperature. The term “stage I survey” in the figure refers to testing done in stage I to establish if there were detectable differences between creep frames. Because of an error in testing, two samples were run at 800 °C (1472 °F) using the stress for the 650 °C (1202 °F) tests. Both samples failed upon loading. The limited results obtained are reported in Table XIII but are not used in any statistical comparisons. Enough data points for the temperature gradients and sample temperature were gathered during the preloading period to provide meaningful data.

Visual observation from Figure 14 suggests that Brew frames 2, 3, and 4 were equal. To confirm this, the creep rate and creep life data for each frame were analyzed statistically to determine if there was a difference in the data sets. A one-way ANOVA was attempted, but the data sets all lacked constant variance, so a Kruskal-Wallis one-way analysis of variance by ranks was used instead. This method generates a test statistic  $H$  and determines if it is sufficiently large to reject the null hypothesis that the data from all three Brew frames are equivalent. The distribution of the actual data is used for small data sets such as these to determine a critical value for  $H$ .

TABLE XIII.—GRCop-84 CREEP RESULTS AFTER MODIFICATIONS

Run	Brew frame	Sample	Set-point temperature, °C	Actual stress, MPa	Life, h	Creep rate, s <sup>-1</sup>	Elongation, percent	Temperature measured by various thermocouples, °C			
								Top	Middle	Bottom	Old control
Vacuum tests											
1	2	1	500	105.8	11.2	1.8×10 <sup>-6</sup>	8.4	513.0	498.7	512.3	438.9
2	2	2	500	105.2	17.5	1.1×10 <sup>-6</sup>	8.5	497.2	502.2	504.1	432.5
7	3	7	500	106.4	10.4	1.2×10 <sup>-6</sup>	5.5	496.8	499.6	502.1	491.9
8	3	8	500	105.2	26.6	8.5×10 <sup>-7</sup>	11.8	502.0	501.8	506.9	499.4
13	4	13	500	105.5	21.0	8.2×10 <sup>-7</sup>	14.7	495.4	497.6	509.8	447.2
14	4	14	500	105.6	31.8	6.6×10 <sup>-7</sup>	15.2	494.5	497.3	500.3	441.6
3	2	3	650	44.2	13.7	1.3×10 <sup>-6</sup>	9.3	645.3	653.1	651.4	603.5
4	2	4	650	44.5	10.7	1.6×10 <sup>-6</sup>	8.6	639.6	649.2	654.0	609.2
9	3	9	650	44.9	14.6	1.1×10 <sup>-6</sup>	9.4	640.3	649.0	651.7	648.9
10	3	10	650	44.2	7.1	1.6×10 <sup>-6</sup>	7.2	643.2	651.5	653.3	653.2
15	4	15	650	43.9	7.2	2.5×10 <sup>-6</sup>	18.0	645.9	651.9	656.9	600.2
16	4	16	650	44.3	10.3	1.6×10 <sup>-6</sup>	15.4	638.1	647.9	653.3	600.7
<sup>a</sup> 5	2	5	800	44.5	0.1	1.4×10 <sup>-3</sup>	49.5	790.9	799.8	804.1	778.8
6	2	6	800	16.9	111.4	7.1×10 <sup>-8</sup>	6.8	791.5	800.5	806.4	781.5
11	3	11	800	16.8	135.9	6.1×10 <sup>-8</sup>	9.1	793.4	798.9	797.2	797.9
12	3	12	800	16.9	12.2	1.3×10 <sup>-6</sup>	12.1	792.1	798.8	798.1	805.0
17	4	17	800	16.9	356.2	4.4×10 <sup>-8</sup>	22.1	790.5	797.6	805.3	761.2
18	4	18	800	16.6	33.6	4.7×10 <sup>-7</sup>	20.6	792.6	799.4	804.8	754.7
Helium atmosphere tests											
1	2	1	500	105.5	7.2	3.5×10 <sup>-6</sup>	11.2	509.0	500.4	493.6	507.0
2	2	2	500	105.4	6.4	3.80×10 <sup>-6</sup>	10.7	505.6	500.3	492.1	505.8
7	3	3	500	104.8	11.7	3.4×10 <sup>-6</sup>	27.7	497.1	499.0	500.6	501.0
8	3	4	500	105.5	7.0	4.2×10 <sup>-6</sup>	13.9	496.3	500.7	501.2	504.9
13	4	5	500	105.7	7.9	4.1×10 <sup>-6</sup>	14.0	491.1	498.2	499.9	456.7
14	4	6	500	104.8	8.8	4.0×10 <sup>-6</sup>	16.2	494.5	500.2	501.1	461.9
3	2	7	650	44.5	7.3	1.4×10 <sup>-6</sup>	5.4	655.9	649.5	636.8	653.0
4	2	8	650	44.7	5.3	2.1×10 <sup>-6</sup>	5.7	658.6	650.1	637.3	656.3
9	3	9	650	44.3	7.8	2.2×10 <sup>-6</sup>	9.0	648.4	649.5	652.2	654.6
10	3	10	650	44.1	7.1	2.4×10 <sup>-6</sup>	9.1	646.5	650.4	649.1	650.7
15	4	11	650	44.3	10.9	1.2×10 <sup>-6</sup>	7.6	647.8	652.2	654.7	603.5
16	4	12	650	44.7	11.9	1.0×10 <sup>-6</sup>	6.9	644.8	650.0	651.9	601.9
<sup>a</sup> 5	2	13	800	44.7	0.1	(b)	40.6	799.6	800.3	795.9	797.0
6	2	14	800	17.6	16.5	4.26×10 <sup>-7</sup>	5.8	797.8	797.2	794.3	797.0
11	3	15	800	17.6	6.0	1.4×10 <sup>-6</sup>	4.6	799.5	801.0	800.4	804.1
12	3	16	800	17.6	11.1	7.0×10 <sup>-7</sup>	4.2	798.9	801.1	801.5	805.7
17	4	17	800	16.5	56.6	1.3×10 <sup>-7</sup>	4.1	793.1	801.3	801.9	752.4
18	4	18	800	17.3	22.0	4.3×10 <sup>-7</sup>	5.2	798.4	802.2	802.3	754.2

<sup>a</sup>Sample failed prematurely upon loading because of the wrong test load.

<sup>b</sup>Not determined.

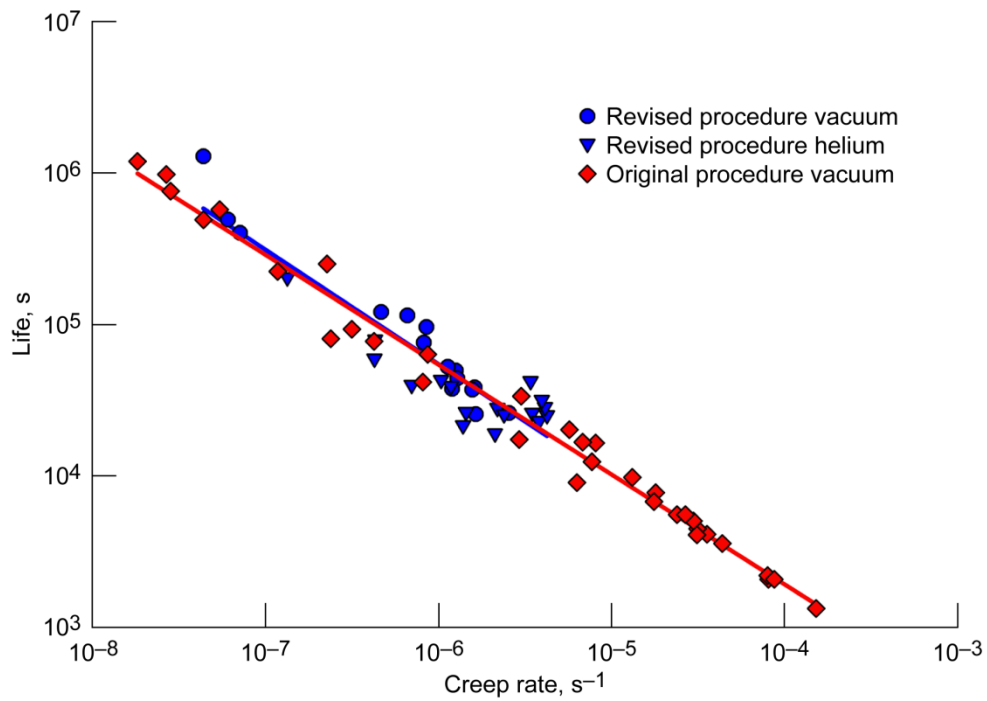


Figure 13.—Creep life versus creep rate for all tests. Revised creep procedure data: life =  $10^{0.20}$  rate<sup>-0.76</sup>; coefficient of determination,  $R^2 = 0.8641$ . Original creep procedure data: life =  $10^{0.38}$  rate<sup>-0.73</sup>;  $R^2 = 0.9851$ .

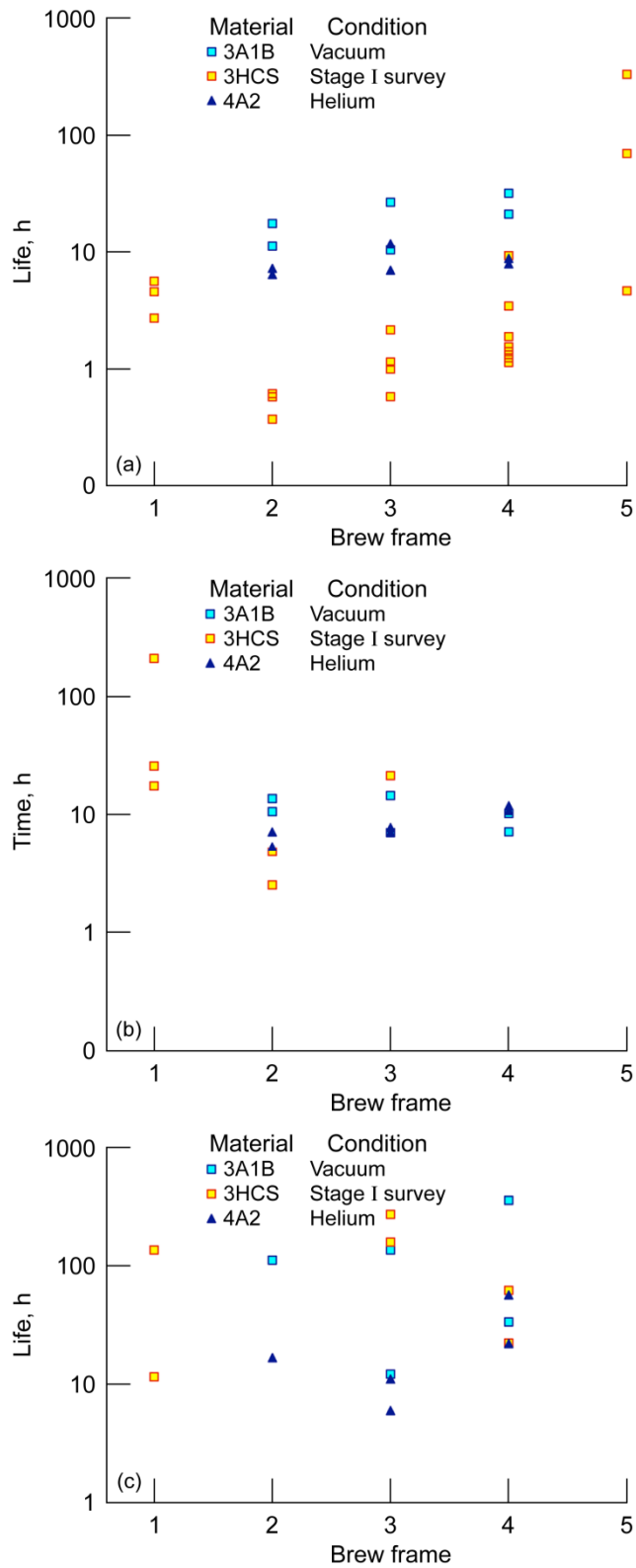


Figure 14.—Creep life. (a) At 500 °C/105 MPa (932 °F/15.2 ksi). (b) At 650 °C/44.3 MPa (1202 °F/6.4 ksi). (c) At 800 °C/17 MPa (1472 °F/2.5 ksi).

Table XIV shows the  $H$  values generated from the statistical analysis and the probability  $P$  of falsely rejecting the null hypothesis that all the data sets are equivalent. The lower the value of  $P$ , the greater the probability that the data sets are different. A lower limit of 0.05 was selected for  $P$  to give a 95-percent confidence in accepting the null hypothesis. In all cases, the analysis indicated that the data sets were statistically equal, but the analysis for the creep rate at 650 °C (1202 °F) in helium has a  $P$  value of only 0.067. This indicates that the data are very close to being statistically significantly different.

On the basis of this analysis, Brew frames 2, 3, and 4 produced statistically equal results for creep rate and creep life in the same environment. This allowed the data sets for each test temperature for both environments to be pooled into two data sets for each test temperature. The averages of the data sets were compared using a  $t$ -test to determine if they were statistically equal. If the tests for normality or equal variance failed, the data sets were compared using a Mann-Whitney Rank Sum Test. Table XV shows the results. The 500 °C (932 °F) data show a difference between the vacuum and helium creep rate and creep life, but the 650 °C (1202 °F) and 800 °C (1472 °F) data sets are statistically equal.

TABLE XIV.—STATISTICAL RESULTS FOR COMPARISON OF BREW FRAMES

[Two degrees of freedom.]

Property	Test temperature, °C	Test statistic, $H$	Equal?	Probability, $P$
Vacuum tests				
Creep life	500	2.000	Yes	0.533
	650	1.143	Yes	.667
	800	.400	Yes	.933
Creep rate	500	3.714	Yes	.200
	650	2.258	Yes	.533
	800	.400	Yes	.933
Helium atmosphere tests				
Creep life	500	2.000	Yes	0.533
	650	3.714	Yes	.200
	800	3.600	Yes	.200
Creep rate	500	1.143	Yes	.667
	650	4.571	Yes	.067
	800	3.000	Yes	.330

TABLE XV.—STATISTICAL COMPARISON OF AVERAGE VACUUM AND HELIUM CREEP PROPERTIES

(a) Creep life.

Test temperature		Normality	Equal variance	Average/median of $\log_{10}(\text{life})$		Equal?	Probability, $P$
°C	°F			Vacuum	Helium		
500	932	Pass	Pass	1.275	0.903	No	0.001
650	1202	Fail	-----	0.935	0.878	Yes	0.937
800	1472	Pass	Pass	1.869	1.227	Yes	0.066

(b) Creep rate.

Test temperature		Normality	Equal variance	Average/median of $\log_{10}(\text{life})$		Equal?	Probability, $P$
°C	°F			Vacuum	Helium		
500	932	Pass	Fail	-6.015	-5.456	No	0.002
650	1202	Fail	-----	-5.796	-5.766	Yes	0.589
800	1472	Pass	Pass	-6.787	-6.326	Yes	0.205

The higher creep rate and shorter life of the helium environment samples was unexpected since the average temperature of the helium specimens was 2.8 °C (5.0 °F) lower and the average gradient was 5.2 °C (9.4 °F) less. With six samples in each data set, the sample size should not have played a major role. The cause for this difference remains unknown and will need to be investigated further in the future.

The helium tests shown in Table XIII did not show a clear benefit for helium over the vacuum in reducing the specimen temperature gradient as was expected. It is likely that small differences in furnace construction and/or geometry between each Brew frame had the biggest remaining effect on the observed temperature gradients.

The creep rates for all tests are plotted by Brew frame at each test temperature in Figure 15. As expected from the strong dependency of the life on rate, after the modifications, all Brew frames have very similar averages and ranges for both the vacuum and helium tests. Data from the stage I tests also are shown in the plots and are designated “stage I survey.” In addition, the creep rates independently determined by step loading at 500, 525, 550, 650, 675, and 700 °C (932, 977, 1022, 1202, 1247, and 1292 °F) are shown in the plots. After the modifications, there was good agreement between creep rates determined by constant loading and step loading. The comparison of creep rates also gives an indication of the actual specimen temperature for the stage I tests. The survey creep rate can be compared with the creep rates determined by step loading at the various temperatures. It is likely that the survey sample was near the temperature with an equal creep rate. The comparisons indicate that the survey samples were generally hotter than the setpoints. These differences in temperature are consistent with the results from the stage II measurement of specimen temperatures.

The creep curves shown in Figure 16 for vacuum tests and in Figure 17 for helium now have similar shapes and magnitudes, confirming that the test conditions are as close to identical as is practical to achieve in the Brew frames. This is in sharp contrast to Figure 9, where there is no consistency in the creep curves. The remaining small differences are explained mostly by the slight variation in specimen temperature, the temperature gradient along the specimen, and inherent material and testing variability.

**GRCop-84 plate testing.**—The results for the vacuum creep testing of GRCop-84 plate made from –140 mesh powder are plotted in Figures 18 and 19. With the larger number of tests and the wider range of stresses, a more accurate assessment of the remaining variability for the creep properties can be made.

Unlike the 2 orders of magnitude scatter for the survey creep test and the 4 orders of magnitude scatter for the combined historical data (Fig. 2), the new data set has a scatter of less than 1 order of magnitude for both the creep rate and the creep life. Even the two-sided 95-percent confidence interval (dashed lines in figures) has a range of less than 1 order of magnitude now.

The creep rate determined using TM–4 for GRCop-84 plate, which was presented in Figure 12, is also plotted in Figure 18. The Brew frame results show excellent agreement with the data for TM–4 and a similar scatter. This reinforces the concept of using TM–4 as a standard. It also demonstrates the ability to generate reproducible and consistent data among multiple Brew frames using the updated creep-testing procedures.

The improved data set was used to quantitatively estimate the dependency of the creep rate and creep life on stress and temperature. The model presented in Equation (1) was examined first with forward stepwise regression. Problems were encountered with the statistical analysis program because both the  $\log_{10}(\sigma)$  and  $1/(T + 273)$  terms had equal  $F$  values to enter. Backward stepwise regression was used to examine the model. The  $\log_{10}(\sigma)/(T + 273)$  term was eliminated in the first step, and the  $\log_{10}(\sigma)$  and  $1/(T + 273)$  terms were both determined to still be statistically significant in the second step. Since the model was reduced to two first-order terms and there were concerns about potential multicollinearity, multilinear regression analysis was conducted using the two remaining variables.

Table XV presents the results of the multilinear regression analysis. The regression analysis suffers from multicollinearity of the independent variables (temperature and stress) as measured by the variance inflation factor (VIF). A VIF value greater than 4 is generally an indication of multicollinearity, and both regression analyses have VIFs of 22.8 for both variables.

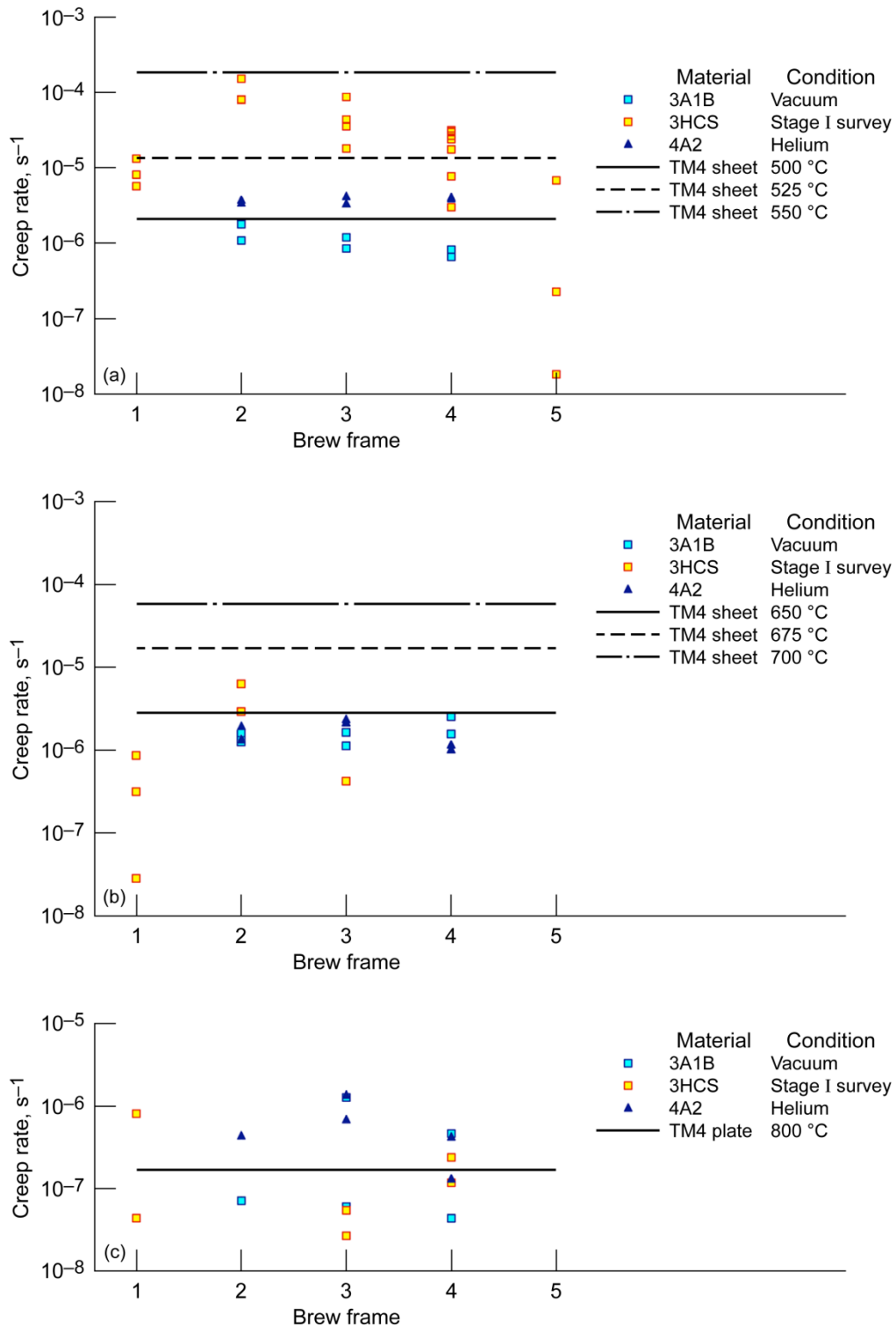


Figure 15.—Creep rate. (a) At 500 °C/105 MPa (932 °F/15.2 ksi). (b) At 650 °C/44.3 MPa (1202 °F/6.4 ksi). (c) At 800 °C/17 MPa (1472 °F/2.5 ksi).

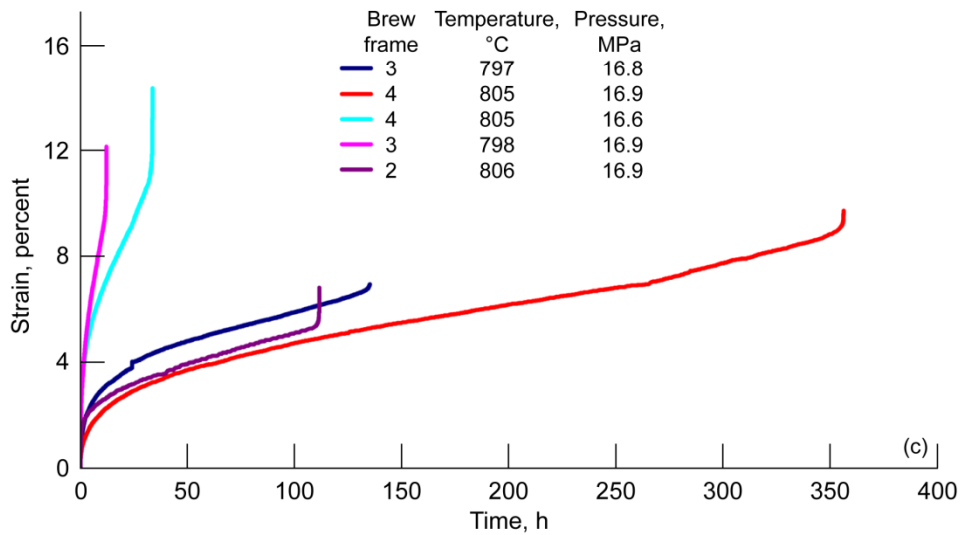
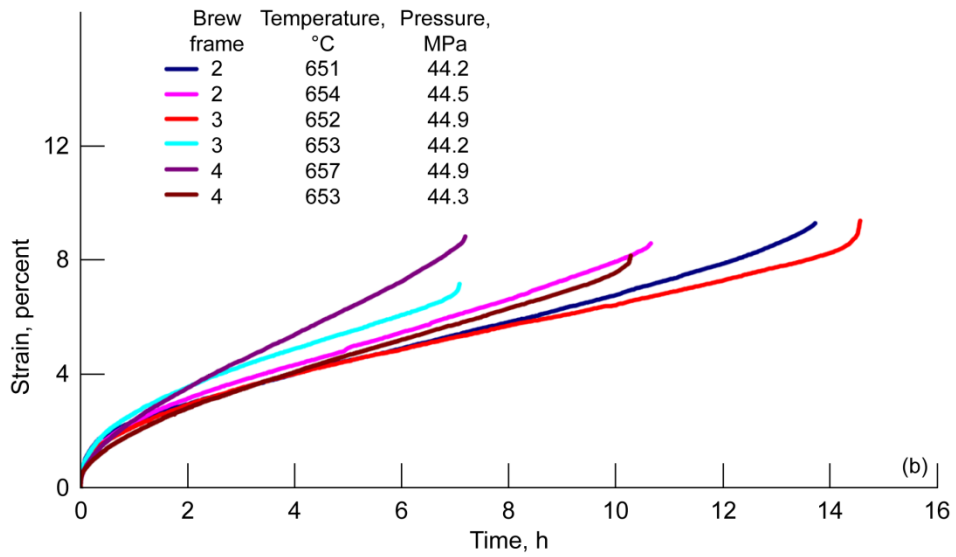
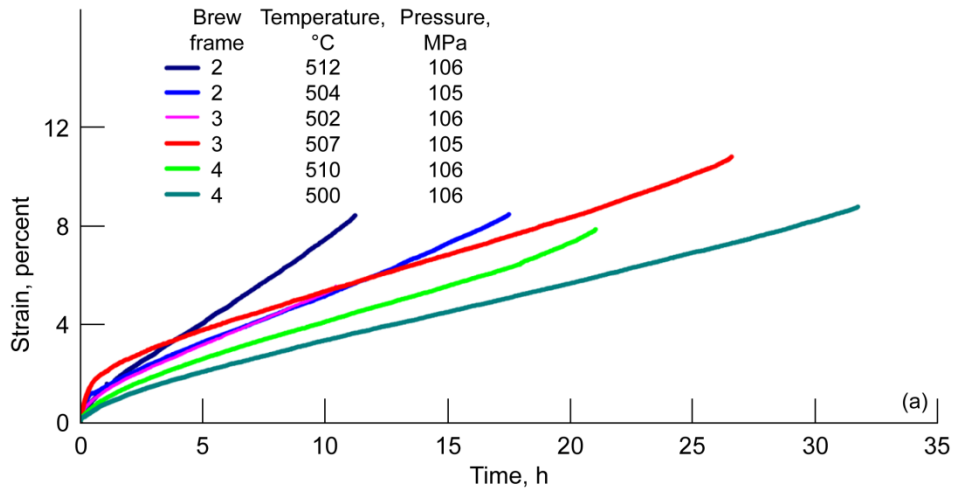


Figure 16.—Creep curves determined in vacuum after Brew frame upgrade.  
 (a) At 500 °C/105 MPa (932 °F/15.2 ksi). (b) At 650 °C/44.3 MPa (1202 °F/6.4 ksi).  
 (c) At 800 °C/17 MPa (1472 °F/2.5 ksi).

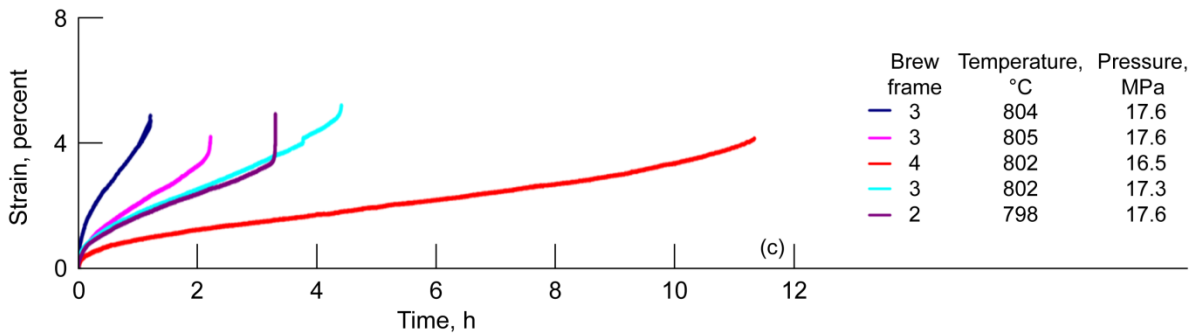
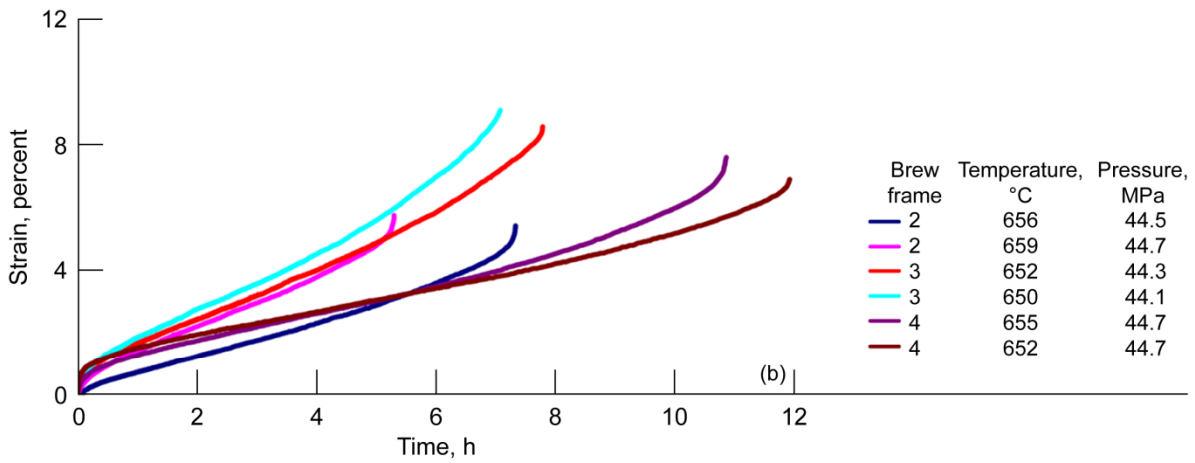
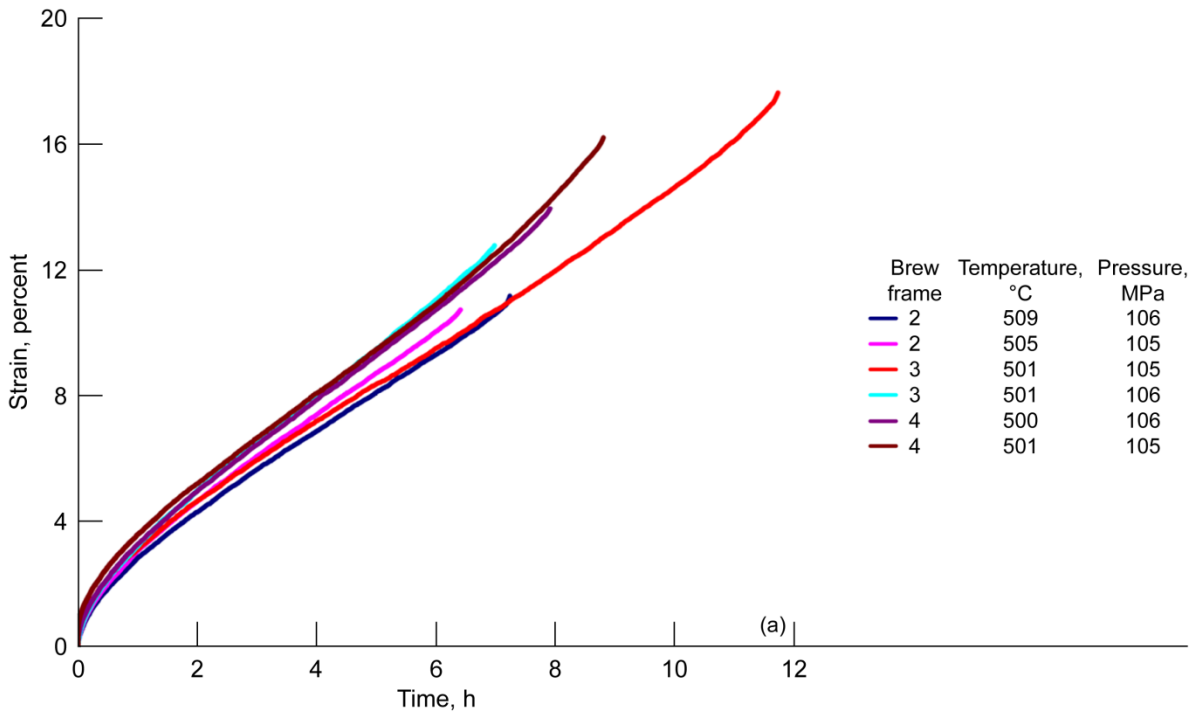


Figure 17.—Creep curves determined in helium atmosphere after Brew frame upgrade. (a) At 500 °C/105 MPa (932 °F/15.2 ksi). (b) At 650 °C/44.3 MPa (1202 °F/6.4 ksi). (c) At 800 °C/17 MPa (1472 °F/2.5 ksi).

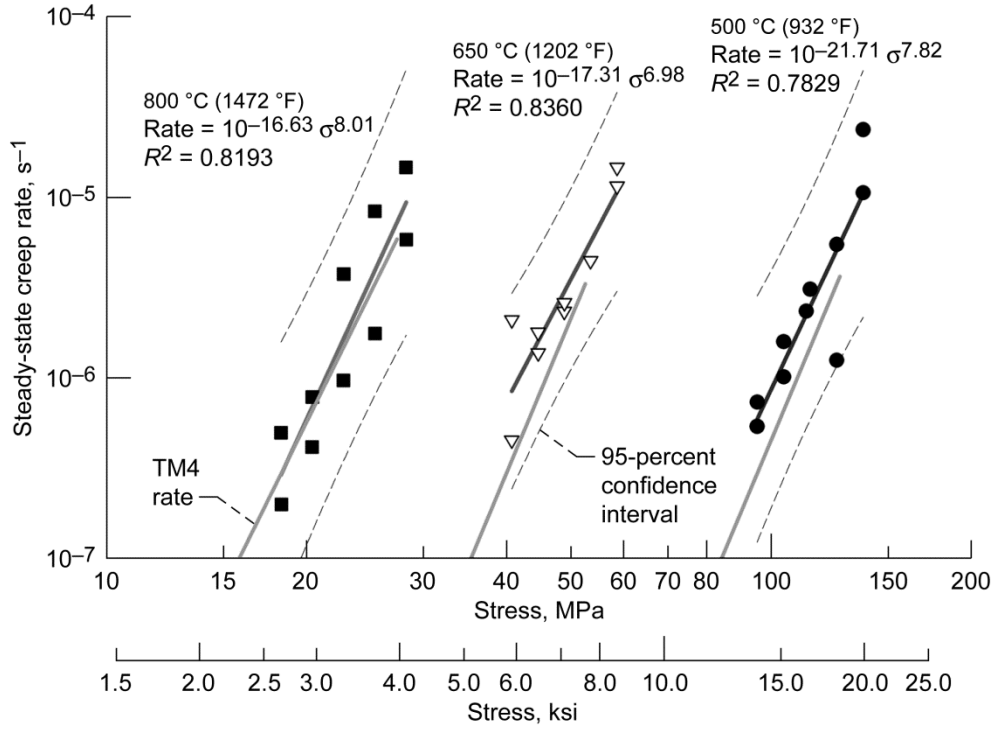


Figure 18.—Creep rate at three different temperatures for GRCop-84 plate made from -140-mesh powder;  $\sigma$ , applied stress;  $R^2$ , coefficient of determination.

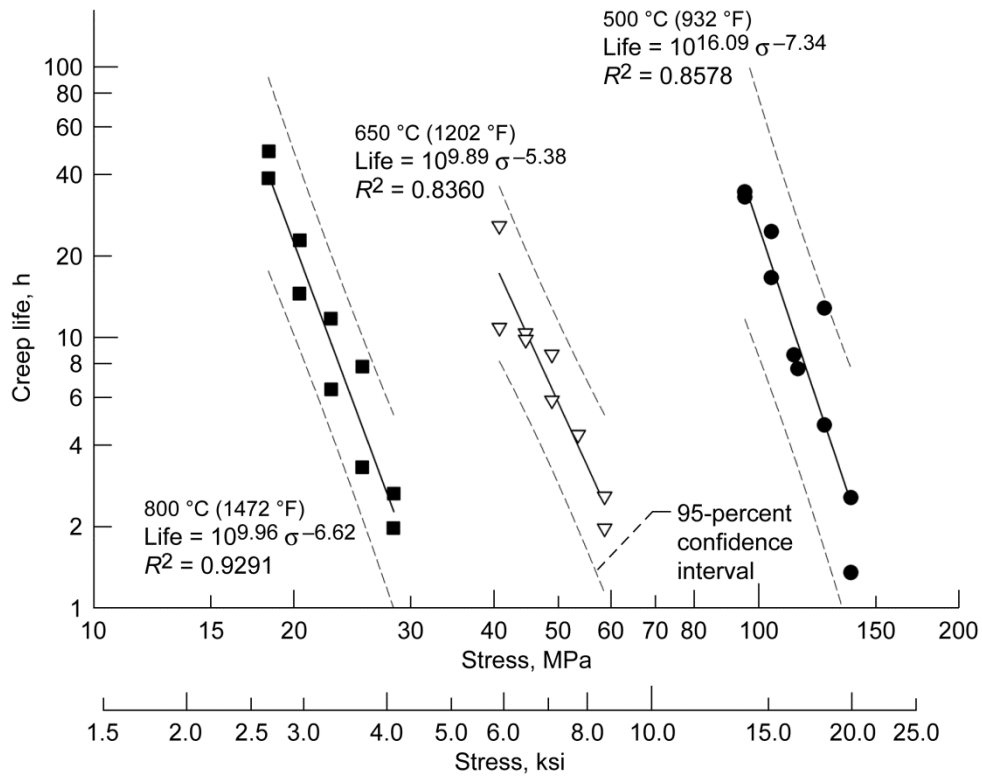


Figure 19.—Creep lives at three different temperatures for GRCop-84 plate made from -140-mesh powder;  $\sigma$ , applied stress;  $R^2$ , coefficient of determination.

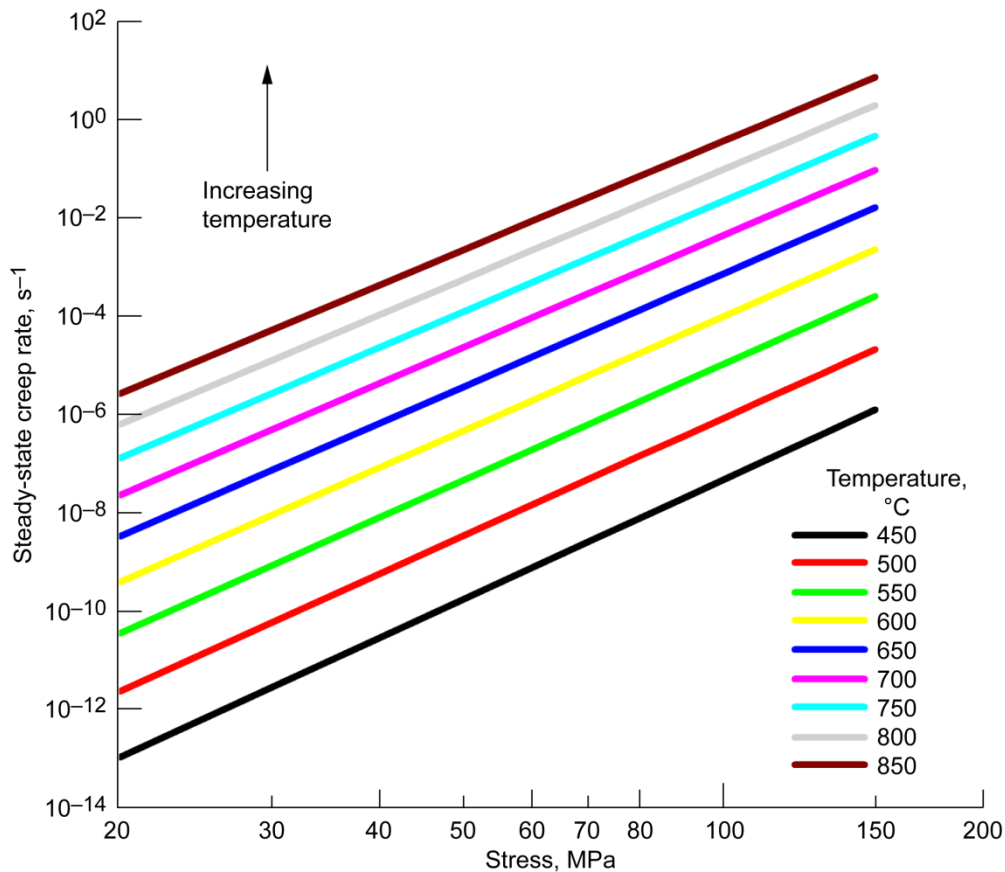


Figure 20.—Dependency of GRCop-84 creep rate on stress at various temperatures.

The multicollinearity was caused by the need to limit the stress range within each test temperature to achieve tests with reasonable durations. As a result, there is a lack of overlap in the stresses at different temperatures and a strong correlation of stress to temperature in the data set. It was decided to still use the regression so that the relative effects of changes in temperature and stress could be assessed.

Figure 20 presents the calculated creep rate as a function of stress at a series of temperatures ranging from 450 to 850 °C. At any given stress, increasing the temperature increases the creep rate as expected. The largest changes are experienced at the lowest temperatures. In the plot, this is manifested as the lines becoming closer together as the temperature increases. A 50 °C increase from 500 to 550 °C increases the creep rate by approximately 1 order of magnitude. The effect decreases as the temperature increases, and the creep rate increases by only about 1/2 order of magnitude when the temperature increases from 800 to 850 °C. The effect of temperature is relatively insensitive to the magnitude of the applied stress.

Figure 21 presents the calculated creep rate as a function of temperature for a series of stresses. As would be expected, the creep rate increases when the stress increases. However, it takes a very large change in stress to change the creep rate by 1 order of magnitude even at the lowest stresses used in this series of creep tests. At the higher stresses, the creep rate is relatively insensitive to even a 10-MPa (1.4-ksi) change in stress.

Typically the applied stress is within 1 MPa (0.1 ksi) or less of the desired stress and is always calculated using the actual load for each test. The lines in Figure 21 represent 10-MPa steps. On the basis of this analysis and the observed consistency of the applied stresses, the effect of small stress differences due to frictional losses and other minor mechanical differences on creep rate will be minimal. The magnitude of the effect of stress is also relatively insensitive to the creep test temperature.

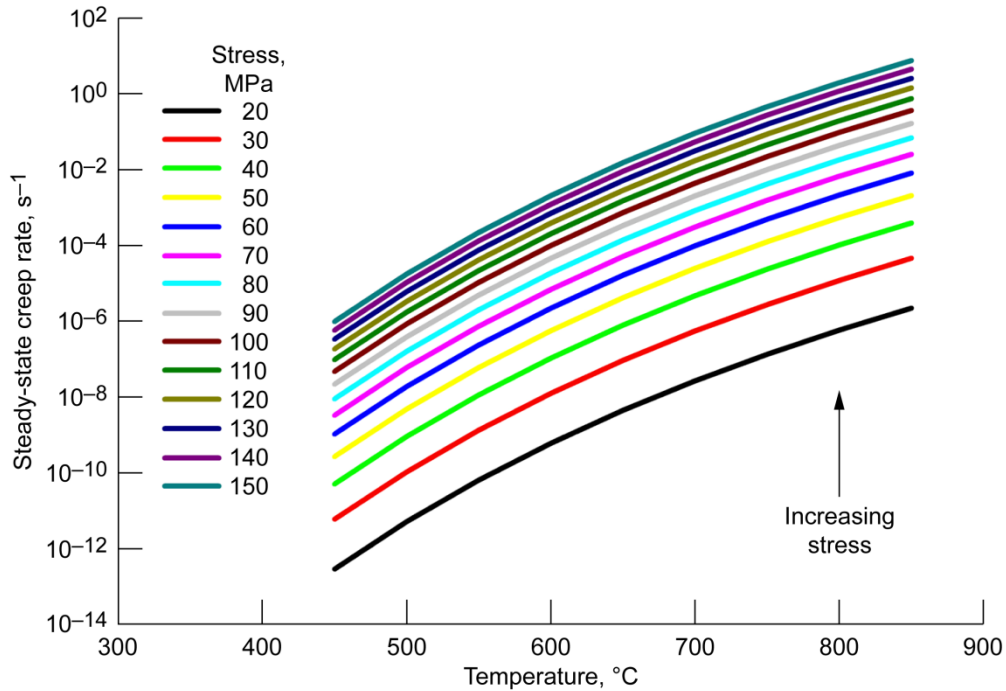


Figure 21.—Dependency of GRCop-84 creep rate on temperature at various stresses.

Creep life follows the same trends, with the life being relatively insensitive to small changes in stress but very sensitive to small changes in temperature. This is consistent with the observations of the testing to determine the sources of variation in creep properties.

The average difference between the chamber thermocouple, which historically served as the specimen temperature control thermocouple, and the middle thermocouple, which now serves as the control thermocouple, was calculated at each temperature for this data set. The average gradients along the sample length also were calculated. The summary is listed in Tables XVI and XVII.

TABLE XVI.—CREEP RATE RESULTS OF MULTILINEAR REGRESSION ANALYSIS

(a) Summary.

Number of observations, $N$ .....	29
Multiple correlation coefficient, $R$ ..	0.899
Standard error of estimate, $S_{Y,X}$ .....	0.243
Missing observations .....	1
Coefficient of determination, $R^2$ ....	0.808
Adjusted $R^2$ .....	0.793

(b) Coefficients determined by multilinear regression, where  $T$  is temperature and  $\sigma$  is stress.

	Coefficient	Standard error	$t$ -Test value	Probability	Variance inflation factor
Constant	-2.924	0.455	-6.426	<0.001	-----
$1/(T - 273)$	-13982.578	1425.634	-9.808	<0.001	22.782
$\log_{10}(\sigma)$	7.471	0.722	10.343	<0.001	22.782

(c) Analysis of variance.

	Degrees of freedom	Sum of squares	Mean square	F value <sup>a</sup>	Probability, P
Regression	2	6.420	3.210	54.558	<0.001
Residual	26	1.530	0.059	-----	-----
Total	28	7.949	0.284	-----	-----

<sup>a</sup>The value of the *F* distribution for *X* degrees of freedom associated with the numerator and *Y* degrees of freedom associated with the denominator.

(d) Incremental change in sum of squares.

Variable	Sum of squares incremental	Sum of squares marginal
1/( <i>T</i> - 273)	0.125	5.660
log <sub>10</sub> (σ)	6.294	6.294

The dependent variable log<sub>10</sub>(creep rate) can be predicted from a linear combination of the independent variables:

(e) Probability that independent variable should not be included.<sup>a</sup>

Independent variable	Probability
1/( <i>T</i> - 273)	<0.001
log <sub>10</sub> (σ)	<0.001

<sup>a</sup>All independent variables appear to contribute to predicting log<sub>10</sub>(creep rate) for *P* < 0.05.

(f) Assumption checks and power of regression.

Test	Pass or fail?	Probability, P
Normality	Passed	0.723
Constant variance	Passed	0.867

Power of performed test with probability α = 0.050.....1.000

<sup>a</sup>α, the acceptable probability of incorrectly concluding that there is a difference.

TABLE XVII.—CREEP LIFE RESULTS OF MULTILINEAR REGRESSION ANALYSIS

(a) Summary.

Number of observations, <i>N</i> .....	29
Multiple correlation coefficient, <i>R</i> .....	0.938
Standard error of estimate, <i>S</i> <sub><i>Y,X</i></sub> .....	0.1550.243
Missing observations.....	1
Coefficient of determination, <i>R</i> <sup>2</sup> .....	0.879
Adjusted <i>R</i> <sup>2</sup> .....	0.870

(b) Coefficients determined by multilinear regression, where *T* is temperature and σ is stress.

	Coefficient	Standard error	<i>t</i> Value	Probability	Variance inflation factor
Constant	-1.838	0.291	-6.320	<0.001	-----
1/( <i>T</i> + 273)	12292.432	911.383	13.488	<0.001	22.782
log <sub>10</sub> (σ)	-6.348	0.462	-13.746	<0.001	22.782

(c) Analysis of variance.

	Degrees of freedom	Sum of squares	Mean square	<i>F</i> value <sup>a</sup>	Probability, <i>P</i>
Regression	2	4.545	2.272	94.506	<0.001
Residual	26	0.625	0.024	-----	-----
Total	28	5.170	0.185	-----	-----

<sup>a</sup>The value of the *F* distribution for *X* degrees of freedom associated with the numerator and *Y* degrees of freedom associated with the denominator.

(d) Incremental change in sum of squares.

Independent variable	Sum of squares incremental	Sum of squares marginal
1/( <i>T</i> + 273)	0.00118	4.374
log <sub>10</sub> (σ)	4.544	4.544

The dependent variable log<sub>10</sub>(life) can be predicted from a linear combination of the independent variables:

(e) Probability that independent variable should not be included.<sup>a</sup>

Independent variable	Probability
1/( <i>T</i> + 273)	<0.001
log <sub>10</sub> (σ)	<0.001

<sup>a</sup>All independent variables appear to contribute to predicting log<sub>10</sub>(life) for *P* < 0.05.

(f) Assumption checks and power of regression.

Test	Pass or fail?	Probability, <i>P</i>
Normality	Passed	0.788
Constant variance	Passed	0.186
Power of performed test with probability α = 0.050... 1.000		

<sup>a</sup>Probability α, the acceptable probability of incorrectly concluding that there is a difference.

The average difference between the chamber thermocouple and the middle sample thermocouple was 12 °C (22 °F), but examination of the differences for the individual Brew frames shows that Brew frame 3 had a very small difference at all temperatures, whereas Brew frame 2 had a much larger difference at all temperatures. Only one test was conducted in Brew frame 4, but it also had a large difference between the chamber and middle thermocouples. In general, the differences decreased with increasing test temperature. The authors believe that this was caused by radiative heating becoming more effective as the test temperature increased and produced more uniform and consistent heating.

As can be seen in Figure 20, such a difference between the specimen temperature and the control thermocouple would have resulted in the sample creeping almost 1 order of magnitude faster in Brew frames 2 and 4 than in Brew frame 3 if the chamber thermocouple had been used to control the test temperature. This highlights how large a role the observed differences in specimen temperature play in the variability observed in the current and historical GRCop-84 data sets.

The gradients in the sample gauge lengths were larger than desired, with average gradients for individual Brew frames being as high as 13.6 °C (24.5 °F) from the top of the sample to the bottom of the sample. In all cases, the bottom was hotter than the top, which is consistent with prior observations. It was also noted that the majority of the gradient occurred between the bottom and the middle of the sample. Average gradients from the middle to the top of the sample were relatively modest and typically in the 2 to 4 °C (4 to 7 °F) range.

Although not desirable, the consistency of the gradients indicates that they were not a major source of variation in the tests for a given Brew frame and were probably a minor contributor to the combined

variability of tests using several Brew frames. It does highlight the need to improve the heaters to eliminate or minimize the thermal gradients.

On the basis of this data set, it appears that the majority of the specimen-to-specimen and frame-to-frame variability was eliminated by the new test procedures. Improvements in the thermal gradients still observed in the specimens may further improve these results, but the inherent variability of the creep of the material now appears to be the dominant source of variability. As will be demonstrated in the next section, the level of variability is now sufficiently low to detect relatively small changes in the creep properties of GRCop-84 caused by processing using statistical analysis.

**GRCop-42 heat treatment effects.**—A regeneratively cooled rocket engine main combustion chamber liner may be installed into its jacket by brazing the liner into the jacket. Such a brazing operation will result in a small, but definite, decrease in the 0.2-percent-offset yield strength of GRCop-84 and its companion alloy GRCop-42 (Ref. 4). Such a decrease in strength should result in a decrease in creep properties since the material is now being tested at a higher fraction of the yield strength. Prior creep testing has not been able to detect differences in the creep behavior of GRCop-42 or GRCop-84 after a high-temperature simulated braze cycle. A new set of GRCop-42 specimens tested using the improved creep test procedures was examined to determine if statistically significant differences could be discerned. If so, the utility of the creep testing improvements in allowing observation of small differences could be validated.

Figures 22 and 23 present the creep properties of extruded GRCop-42 in the as-extruded and brazed conditions. Visually there are strong indications that the expected trends are occurring. The simulated braze cycles tend to lower life and higher rate, and a 1000 °C (1832 °F) braze cycle results in a larger change than a 935 °C (1715 °F) braze cycle.

To confirm that these apparent trends are correct, a forward stepwise regression using the model presented in Equation 2 was conducted. Again,  $F$  values of 4 to enter and 3.9 to leave were used to determine which variables should be in the model. For both the rate and life models, the  $\log_{10}(\sigma)$  term was marginal for inclusion ( $P = 0.046$  for the creep life model) or exclusion ( $P = 0.059$  for the creep rate model) since the desired  $P$  value is 0.05 for 95-percent confidence. It was decided for consistency between the models that the  $\log_{10}(\sigma)$  term would be excluded from the creep life model. This was not considered to be a major problem even though the stress was known to be a prime determiner of creep rate and life. The stress dependency was instead incorporated in the creep models through the stress-temperature interaction variable ( $\log_{10}(\sigma)/(T + 273)$ ) and through the 935 °C (1715 °F) braze-stress variable ( $B_1 \log_{10}(\sigma)$ ), so that the stress dependency of the creep of GRCop-42 would still be captured. The forward stepwise regression was rerun, and the fit of the model to the data was slightly decreased as shown by the  $R^2$  value decreasing from 0.939 to 0.930. This change was considered to be insignificant, and the model was kept.

Table XVIII presents the ANOVA and  $F$  statistics from the last step of the regression analysis for creep rate and creep life, as well as the coefficients for each variable. The  $P$  values for the variables in the model are the probability of a false positive (the variable is actually not statistically significant but enters the regression model). The  $P$  values for the variables not in the model are the probability that the variable should not be in the model.

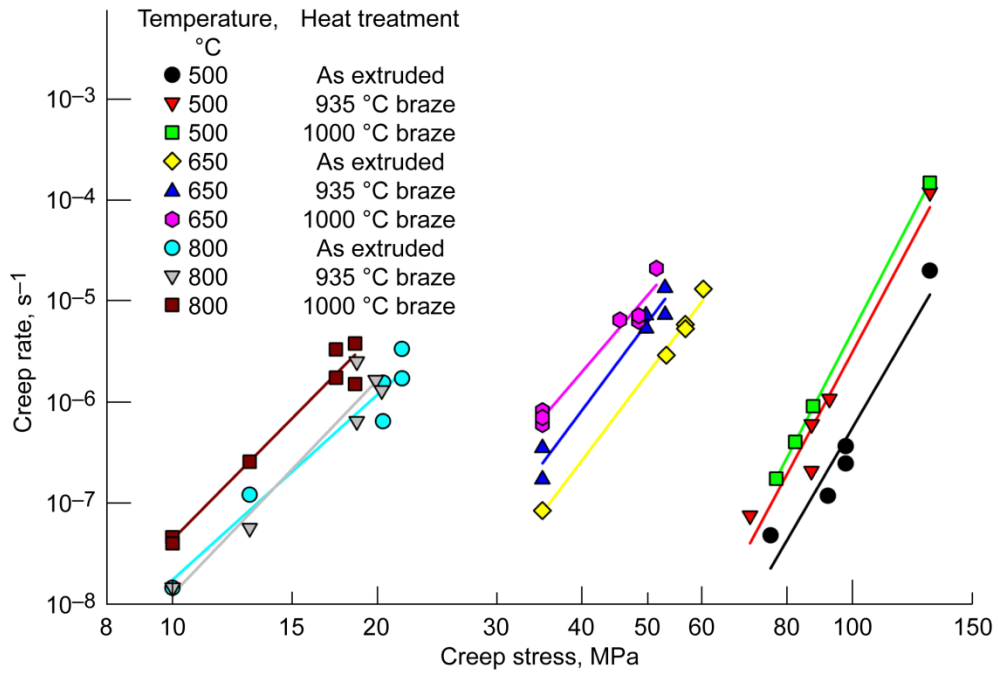


Figure 22.—Creep rates for extruded and brazed GRCop-42 with different heat treatments.

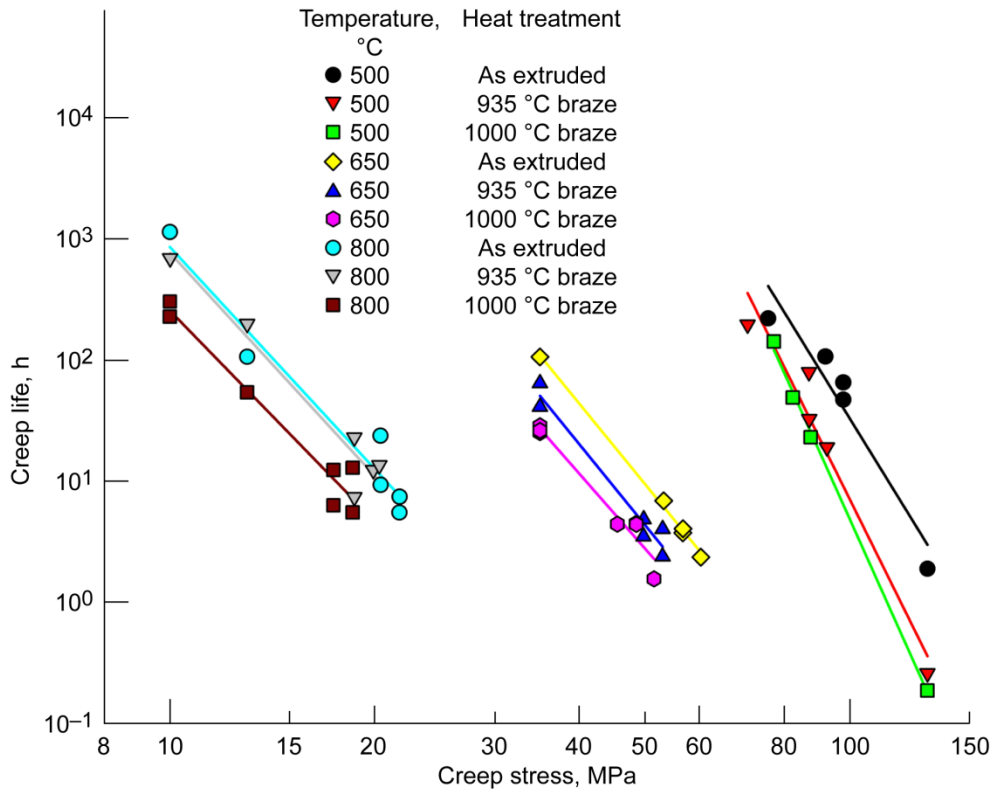


Figure 23.—Creep lives for extruded and brazed GRCop-42 with different heat treatments.

TABLE XVIII.—AVERAGE TEMPERATURE DIFFERENCES AND GRADIENTS  
FOR GRCop-84 TESTS

Temperature		Brew frame	Temperature difference, middle to chamber, °C	Temperature gradient, °C		
°C	°F			Top to bottom	Top to middle	Middle to bottom
All	All	All	12.0	-9.3	-5.7	-3.4
		2	27.6	-12.3	-7.5	-4.2
		3	0.2	-6.9	-4.2	-2.7
		4	25.8	-13.6	-8.7	-4.9
500	932	All	15.4	-8.0	-6.1	-1.9
		2	48.0	-10.2	-8.2	-2.0
		3	4.6	-4.8	-3.0	-1.8
		4	25.8	-13.6	-8.7	-4.9
650	1202	All	17.6	-8.0	-6.1	-1.9
		2	31.4	-10.2	-8.2	-2.0
		3	-3.2	-4.8	-3.0	-1.8
800	1472	All	3.0	-7.2	-4.2	-3.0
		2	11.5	-10.4	-5.6	-4.9
		3	-2.7	-5.0	-3.2	-1.8

In examining the statistically important variables, the influence of the simulated braze cycle on creep rate and creep life is now strongly statistically significant as demonstrated by the inclusion of variables with the blocking variables ( $B_1$ ,  $B_2$ ) and their large  $F$  values. Furthermore, the effects of the simulated braze cycle can be quantified through the coefficients of the models.

These results are in direct contrast to historical efforts (Ref. 2, to be published, and Ref. 4), which could not detect a statistically significant effect for heat treatments including the simulated braze cycles. It clearly demonstrates the improvements in both the experimental procedures and the quality and utility of the creep results from Brew frame creep tests. It also demonstrates that data from multiple Brew frames can be used to detect these small differences.

As with the GRCop-84 plate data set, the average temperature difference and gradients were calculated. The results appear in Tables XIX and XX. Brew frames 2 and 4 have a sample temperature far higher than the chamber thermocouple previously used for control. Brew frame 3 has nearly the same temperature reading from both thermocouples. The difference between the chamber and middle sample thermocouples can average as much as 42.2 °C. For Brew frame 2, the difference decreased with increasing temperature as was observed for the GRCop-84 plate samples. However, Brew frame 4 did not have the same trend. If radiative heat transfer was becoming more effective in Brew frame 2 and was reducing the difference, it would be expected that the same trend would be observed in Brew frame 4. The lack of such a trend suggests that another, unknown mechanism might have been operative and that there might have been a lurking variable not in the model or analyses. For now the analysis of the creep properties indicates that the variable does not have a large enough effect to prevent good analysis of the test results.

TABLE XIX.—STATISTICAL ANALYSIS OF GRCop-42 CREEP RATE

(a) Summary

Number of observations, $N$ .....	50
Multiple correlation coefficient, $R$ .....	0.969
Standard error of estimate, $S_{Y,X}$ .....	0.238
Coefficient of determination, $R^2$ .....	0.939
Adjusted $R^2$ .....	0.934

(b) Analysis of variance.

Group	Degrees of freedom	Sum of squares	Mean square	$F$ value <sup>a</sup>	Probability, $P$
Regression	4	40.093	10.023	177.208	<0.001
Residual	46	2.602	0.0566	-----	-----

<sup>a</sup>The value of the  $F$  distribution for  $X$  degrees of freedom associated with the numerator and  $Y$  degrees of freedom associated with the denominator.

(c) Variables in model, where  $T$  is temperature,  $\sigma$  is stress, and  $B_1$  and  $B_2$  are the blocking variables corresponding to brazes of 935 and 1000 °C, respectively.

Variable	Coefficient	Standard error	$F$ value <sup>a</sup>	Probability
Constant	13.192	0.808	-----	-----
$1/T + 273$	-30765.830	1224.541	631.234	<0.001
$\log_{10}(\sigma)/(T + 273)$	7868.689	302.107	678.397	<0.001
$B_2/(T + 273)$	692.479	76.833	81.230	<0.001
$B_1 \log_{10}(\sigma)$	0.285	0.0507	31.504	<0.001

(d) Variables not in model.

Variable	Coefficient	Standard error
$\log_{10}(\sigma)$	3.754	0.059
$B_1/(T + 273)$	1.337	0.254
$B_2 \log_{10}(\sigma)$	0.106	0.746

(e) Assumption checks and power of regression.

Test	Pass or fail?	Probability, $P$
Normality	Passed	0.358
Constant variance	Passed	0.859
Power of performed test with probability $\alpha = 0.050$ ..... 1.000		

<sup>a</sup>Probability  $\alpha$ , the acceptable probability of incorrectly concluding that there is a difference.

TABLE XX.—STATISTICAL ANALYSIS OF GRCop-42 CREEP LIFE

(a) Summary.

Number of observations, $N$ .....	50
Multiple correlation coefficient, $R$ .....	0.966
Standard error of estimate, $S_{Y,X}$ .....	0.220
Coefficient of determination, $R^2$ .....	0.930
Adjusted $R^2$ .....	0.924

(b) Analysis of variance.

Group	Degrees of freedom	Sum of squares	Mean square	$F$ value <sup>a</sup>	Probability, $P$
Regression	4	29.737	7.434	153.936	<0.001
Residual	46	2.222	0.0483	-----	-----

<sup>a</sup>The value of the  $F$  distribution for  $X$  degrees of freedom associated with the numerator and  $Y$  degrees of freedom associated with the denominator.

(c) Variables in model, where  $T$  is temperature,  $\sigma$  is stress, and  $B_1$  and  $B_2$  are the blocking variables corresponding to brazes of 935 and 1000 °C, respectively.

Variable	Coefficient	Standard error	$F$ value <sup>a</sup>	Probability
Constant	-15.593	0.746	-----	-----
$1/T + 273$	26866.373	1131.508	563.771	<0.001
$\log_{10}(\sigma)/(T + 273)$	-6830.686	279.155	598.741	<0.001
$B_2/(T + 273)$	-543.622	70.996	58.631	<0.001
$B_1 \log_{10}(\sigma)$	-0.231	0.0469	24.221	<0.001

(d) Variables not in model.

Variable	Coefficient	Standard error
$B_1/(T + 273)$	0.803	0.375
$B_2 \log_{10}(\sigma)$	0.202	0.655
$\log_{10}(\sigma)$	Excluded from model	

(e) Assumption checks and power of regression.

Test	Pass or fail?	Probability, $P$
Normality	Passed	0.277
Constant variance	Passed	0.840
Power of performed test with probability $\alpha = 0.050$ ..... 1.000		

<sup>a</sup>Probability  $\alpha$ , the acceptable probability of incorrectly concluding that there is a difference.

The temperature gradients along the gauge section of the specimens were again higher than desired, as shown in Table XXI. The average gradients were as high as 22.1 °C (39.8 °F), and overall they averaged 12.5 °C (22.5 °F) from the top to the bottom of the sample. Although the maximum gradient exceeds that observed for the GRCop-84 specimens, the overall average is similar to the overall GRCop-84 average gradient of 9.3 °C (16.7 °F).

The average gradients for the individual Brew frames at each test temperature were examined next. The results for Brew frames 3 and 4 were generally consistent with the GRCop-84 plate data set. However, the average gradients for the GRCop-42 specimens tested in Brew frame 2 were nearly twice those of GRCop-84 plate specimens tested in the same frame. The larger gradients in Brew frame 2 were the primary source of the difference in the observed differences in the average gradients at all temperatures. The gradient data for Brew frame 2 may have been influenced by having only five GRCop-42 tests from Brew frame 2 in this data set. The small number of samples with only the 500 °C (932 °F) and 650 °C (1202 °F) test temperatures having a repeat may skew the averages.

Most of the increase in the top-to-bottom gradient occurred between the top and middle thermocouples. The implication of this is that the top section of the specimen was cooler in the GRCop-42 tests than in the GRCop-84 tests. As shown in Figure 20, the lower temperature would result in a lower creep rate, which would also result in a longer creep life. For a 5 to 10 °C (9 to 18 °F) change, the creep rate could decrease by 1/10 to 1/3 order of magnitude. The variation in gradients from data set to data set is undesirable, and it appears to be a contributor to the remaining variability in the data sets. A goal of any new furnace heater design will need to be to not only reduce the gradients overall but to make them consistent from frame to frame so that this source of error is minimized.

In Tables XVIII and XXI, the magnitude of the gradient from the bottom thermocouple to the middle thermocouple normally exceeds that of the gradient from the middle thermocouple to the top thermocouple. These results are consistent with the observations in the prior testing to seek out sources of variability. Because of the consistency of the gradient direction and the difference in magnitude between the top half and the bottom half, the total gradient is reported rather than the middle thermocouple value plus or minus half of the average measured gradient. It is felt that this is a more appropriate and meaningful way to present the data at this point since it captures the asymmetry of the gradient, whereas a single value with a simple plus/minus range does not. If the heater is redesigned and the two gradients are equalized, then the best method of reporting the gradients will be revisited.

TABLE XXI.—AVERAGE TEMPERATURE DIFFERENCES AND GRADIENTS  
FOR GRCop-42 TESTS

Temperature		Brew frame	Temperature difference, middle to chamber, °C	Temperature gradient, °C		
°C	°F			Top to bottom	Top to middle	Middle to bottom
All	All	All	15.9	-12.5	-6.8	-5.8
		2	33.7	-19.3	-14.5	-4.8
		3	-1.6	-7.3	-5.3	-2.1
		4	20.1	-13.7	-6.3	-7.5
500	932	All	21.1	-14.0	-7.4	-6.6
		2	42.2	-22.1	-17.3	-4.8
		3	-0.7	-10.9	-6.6	-4.3
		4	21.2	-13.0	-5.7	-7.3
650	1202	All	16.0	-15.0	-8.5	-6.5
		2	34.5	-21.0	-15.3	-5.7
		3	-2.8	-7.6	-5.7	-1.9
		4	20.4	-16.8	-8.8	-8.0
800	1472	All	11.7	-9.1	-4.6	-4.5
		2	21.7	-12.7	-10.0	-2.7
		3	-1.1	-6.2	-4.6	-1.5
		4	18.7	-10.5	-3.6	-6.9

## Summary and Conclusions

It was shown that significant differences existed between results obtained for five Brew creep test frames when identical specimens with the same process history were tested under presumably identical conditions. It was determined that the primary cause for the variability was that the setpoint control temperature measured by a noncontact thermocouple was different from the actual sample temperature by a large and variable amount.

Equipment and procedure modifications that were implemented resulted in the creep rate between Brew frames now being equivalent to an independently determined calibration standard. The variation decreased to about 1/2 order of magnitude from 2 to 4 orders of magnitude.

Substituting a helium atmosphere for vacuum generally decreased the temperature gradient along the specimen by improving the uniformity of heat transfer from the heater to the specimen. This further decreased variability in the results especially at 500 °C. It does not appear that the helium consistently helped at higher test temperatures.

It was also shown that GRCop-84 creep behavior is much more sensitive to small temperature changes than to small stress changes. This magnified the effects of differences in specimen temperature on test-to-test variability. Higher test-to-test variability increases the total variability observed in the creep properties.

It is probable that most creep tests conducted prior to modifying the creep test methods and procedures were done at sample temperatures higher than reported. The magnitude of the temperature difference may have been as high as 50 °C (90 °F) for some tests. The estimated average temperature difference was approximately 15 °C (27 °F) on the basis of observed temperature differences between the control thermocouple and the middle specimen thermocouple for the GRCop-84 and GRCop-42 tests in this report. The differences varied from frame to frame and were fairly strongly dependent on the test temperature for Brew frame 2 but not very dependent on the test temperature for Brew frames 3 and 4.

These combined findings strongly indicate that previous tests prior to implementing these modifications resulted in reporting GRCop-84 creep lives shorter than the actual value and creep rates greater than the actual values at the reported setpoint temperature. This means that the prior reported work (Ref. 4) is overly conservative. On the basis of the analysis of the dependency of creep rate and creep life

on temperature, the temperature difference is sufficient to increase creep rates by 1/3 to 1 order of magnitude and to decrease creep lives by 1/3 to 1 order of magnitude.

The verification testing in stage III using the updated methods shows that the variability in the creep results has been greatly decreased. The testing was also demonstrated to be enhanced by being able to detect and quantify small differences in creep rate and creep life using statistical analyses. Analysis of GRCop-84 plate specimens showed that the variability for a single material condition was reduced to 1 order of magnitude or less as measured by the 95-percent confidence interval for the regression analysis. Testing GRCop-42 specimens in three conditions demonstrated that small differences in creep behavior previously masked by the large variability in the data were now distinguishable and that quantifiable changes in the creep properties could be calculated. The improvements also imply that smaller numbers of samples will be needed for future testing to accurately characterize the response of GRCop-42, GRCop-84, and other samples tested in these creep frames.

## Future Work

It would be desirable to replace the current wire mesh heaters with solid heaters to determine if they produce smaller thermal gradients as were observed with TM-4. The gradients need to be reduced to  $\pm 5$  °C or less to produce the best possible creep results. Such work is currently not planned but will be proposed in the future.

## References

1. de Groh, Henry C., III; Ellis, David L.; and Loewenthal, William S.: Comparison of GRCop-84 to Other High Thermal Conductive Cu Alloys. NASA/TM—2007-214663, 2007. <http://gltrs.grc.nasa.gov> Accessed Feb. 6, 2009.
2. Ellis, D.L.; Loewenthal, W.S.; and Haller, H.: Creep of Commercially Produced GRCop-84. NASA/TM—2012-216998, 2012, to be published.
3. Ellis, David L.; and Michal, Gary M.: Mechanical and Thermal Properties of Two Cu-Cr-Nb Alloys and NARloy-Z. NASA/CR—198529, 1996. <http://gltrs.grc.nasa.gov> Accessed Feb. 6, 2009.
4. Ellis, D.L.: GRCop-84. Aerospace Structural Materials Handbook Supplement, 40th ed., vol. 6, CINDAS LLC, West Lafayette, IN, 2001.
5. Loewenthal, William S.; and Ellis, David L.: GRCop-84 Rolling Parameter Study. NASA/TM—2008-215213, 2008. <http://gltrs.grc.nasa.gov> Accessed Feb. 6, 2009.
6. ASTM Standard E-8. Standard Test Methods for Tension Testing of Metallic Materials. ASTM International, West Conshohocken, PA, 2008.
7. Ellis, David, et al.: A Practical Guide to the Production of Metal Spun NiCrAlY Coated GRCop-84 Liners. NASA/TM—2006-214123, 2006. Available from the NASA Center for Aerospace Information.
8. Monkman, F.C.; and Grant, N.J.: An Empirical Relationship Between Rupture Life and Minimum Creep Rate in Creep-Rupture Tests. Proc. ASTM, vol. 56, 1956, pp. 593–620.
9. Reed-Hill, Robert E.: Physical Metallurgy Principles. 2nd ed., Van Nostrand, New York, NY, 1973, pp. 871–877.
10. Ellis, D.L.; and Garg, A.: Annealing of GRCop-84. To be published as a NASA TM.

REPORT DOCUMENTATION PAGE			Form Approved OMB No. 0704-0188		
<p>The public reporting burden for this collection of information is estimated to average 1 hour per response, including the time for reviewing instructions, searching existing data sources, gathering and maintaining the data needed, and completing and reviewing the collection of information. Send comments regarding this burden estimate or any other aspect of this collection of information, including suggestions for reducing this burden, to Department of Defense, Washington Headquarters Services, Directorate for Information Operations and Reports (0704-0188), 1215 Jefferson Davis Highway, Suite 1204, Arlington, VA 22202-4302. Respondents should be aware that notwithstanding any other provision of law, no person shall be subject to any penalty for failing to comply with a collection of information if it does not display a currently valid OMB control number.</p> <p>PLEASE DO NOT RETURN YOUR FORM TO THE ABOVE ADDRESS.</p>					
1. REPORT DATE (DD-MM-YYYY) 01-12-2011		2. REPORT TYPE Technical Memorandum		3. DATES COVERED (From - To)	
4. TITLE AND SUBTITLE Sources of Variation in Creep Testing			5a. CONTRACT NUMBER		
			5b. GRANT NUMBER		
			5c. PROGRAM ELEMENT NUMBER		
6. AUTHOR(S) Loewenthal, William, S.; Ellis, David, L.			5d. PROJECT NUMBER		
			5e. TASK NUMBER		
			5f. WORK UNIT NUMBER WBS 599489.02.07.03.02.04.01		
7. PERFORMING ORGANIZATION NAME(S) AND ADDRESS(ES) National Aeronautics and Space Administration John H. Glenn Research Center at Lewis Field Cleveland, Ohio 44135-3191			8. PERFORMING ORGANIZATION REPORT NUMBER E-16689		
9. SPONSORING/MONITORING AGENCY NAME(S) AND ADDRESS(ES) National Aeronautics and Space Administration Washington, DC 20546-0001			10. SPONSORING/MONITOR'S ACRONYM(S) NASA		
			11. SPONSORING/MONITORING REPORT NUMBER NASA/TM-2011-215493		
12. DISTRIBUTION/AVAILABILITY STATEMENT Unclassified-Unlimited Subject Category: 26 Available electronically at <a href="http://www.sti.nasa.gov">http://www.sti.nasa.gov</a> This publication is available from the NASA Center for AeroSpace Information, 443-757-5802					
13. SUPPLEMENTARY NOTES					
14. ABSTRACT Creep rupture is an important material characteristic for the design of rocket engines. It was observed during the characterization of GRCop-84 that the complete data set had nearly 4 orders of magnitude of scatter. This scatter likely confounded attempts to determine how creep performance was influenced by manufacturing. It was unclear if this variation was from the testing, the material, or both. Sources of variation were examined by conducting tests on identically processed specimens at the same specified stresses and temperatures. Significant differences existed between the five constant-load creep frames. The specimen temperature was higher than the desired temperature by as much as 43 °C. It was also observed that the temperature gradient was up to 44 °C. Improved specimen temperature control minimized temperature variations. The data from additional tests demonstrated that the results from all five frames were comparable. The variation decreased to 1/2 order of magnitude from 2 orders of magnitude for the baseline data set. Independent determination of creep rates in a reference load frame closely matched the creep rates determined after the modifications. Testing in helium tended to decrease the sample temperature gradient, but helium was not a significant improvement over vacuum.					
15. SUBJECT TERMS Creep properties; Temperature; Temperature gradients; Variability					
16. SECURITY CLASSIFICATION OF:			17. LIMITATION OF ABSTRACT	18. NUMBER OF PAGES	19a. NAME OF RESPONSIBLE PERSON
a. REPORT	b. ABSTRACT	c. THIS PAGE			STI Help Desk (email:help@sti.nasa.gov)
U	U	U	UU	53	19b. TELEPHONE NUMBER (include area code) 443-757-5802



